CHAPTER ONE: INTRODUCTION

1.1 Background of the Study

1.1.1 Quantum entanglement and Bell states

Quantum entanglement is a physical phenomenon in quantum mechanics that occurs when pairs or groups of particles are generated or interact in such a manner that the quantum state of each particle cannot be described independently; instead, a quantum state is given for the system as a whole. This phenomenon originated from the 1935 paper of Einstein, Podolsky and Rosen (EPR) and produced the EPR paradox which existed until in 1964 when John Bell suggested measuring certain correlations between entangled states. These correlations would violate Bell's inequality if quantum mechanics was correct. Mathematical treatment of quantum mechanics becomes exponentially complicated when it is applied to multiple particles hence most studies of interest have been done on a two-particle system (a bipartite system). Entanglement between two particles occurs when the particles are in a quantum superposition of states, and their states are correlated. Mathematically, a system that could be in one of multiple states is represented as a linear combination of those states. For example, a photon can be in either horizontal polarization state $|H\rangle$ or vertical polarization state $|V\rangle$. The general polarization state vector $|\psi\rangle$ of a photon is given by (Chauser and Shimony, 1978)

$$|\psi\rangle = x|H\rangle + y|V\rangle \qquad (1.0)$$

where x and y are complex numbers which represent probabilities to be in the horizontal or vertical polarization state, respectively, such that

$$|x|^2 + |y|^2 = 1 \qquad (1.1)$$

The photon is therefore said to be in a superposition of horizontal and vertical polarization. The horizontal polarization state vector represents the basic unit vector $|0\rangle$ and the vertical polarization state vector represents the basic unit vector $|1\rangle$ according to the definition

$$|H\rangle = |0\rangle \quad ; \qquad |0\rangle = \begin{pmatrix} 1 \\ 0 \end{pmatrix} \tag{1.2a}$$

$$|V\rangle = |1\rangle \quad ; \qquad |1\rangle = \begin{pmatrix} 0 \\ 1 \end{pmatrix} \tag{1.2b}$$

Entangled photon states are produced from nonlinear parametric processes. In a general parametric process, a beam of radiation called the pump is incident on a befringet crystal. The pump is intense enough so that nonlinear effects lead to conversion of pump photons into pairs of correlated photons. The process is parametric because it depends on electric fields in which energy is conserved. The photons in a parametric process exit the crystal such that one is aligned in a horizontally polarized light cone producing horizontal polarization state $|H\rangle$ while the other is aligned in a vertically polarized light cone producing vertical polarization state $|V\rangle$. Bell states are the most entangled states. Photon entanglement in a parametric process can be studied by constructing Bell state vectors using photon polarization state vectors from a spontaneous parametric down conversion (SPDC) (Ling, 2008).

$$|\psi_+\rangle = \frac{1}{\sqrt{2}}\left(|H\rangle_a |H\rangle_b + |V\rangle_a |V\rangle_b\right) \tag{1.3a}$$

$$|\psi_-\rangle = \frac{1}{\sqrt{2}}\left(|H\rangle_a |H\rangle_b - |V\rangle_a |V\rangle_b\right) \tag{1.3b}$$

$$\left|\Phi_{+}\right\rangle = \frac{1}{\sqrt{2}}\left(\left|H\right\rangle_a\left|V\right\rangle_b + \left|V\right\rangle_a\left|H\right\rangle_b\right) \qquad (1.3c)$$

$$\left|\Phi_{-}\right\rangle = \frac{1}{\sqrt{2}}\left(\left|H\right\rangle_a\left|V\right\rangle_b - \left|V\right\rangle_a\left|H\right\rangle_b\right) \qquad (1.3d)$$

Entanglement has found many applications in the fields of quantum computation and quantum information processing such as quantum cryptography (Ekert, 1991), quantum dense coding (Bennett & Wiesner, 1992), entanglement swapping (Yurke & Stoler, 1992), quantum lithography (Boto & Kok, 1994) and quantum teleportation (Bennett & Brassard, 1993). Quantum teleportation which refers to the transfer of quantum states between distant locations without an intervening medium has been achieved over long distances (Rupert, 2004; Herbst & Scheidl, 2012; Takeda, 2014). China launched the world's first "quantum satellite", a communication system incapable of being hacked and stretching over a distance of 2000km (Adams, 2016). Entangled photons produce continuous variable (CV) systems which provide a good opportunity to study entanglement due to their much larger Hilbert space. In the current work we consider a type of CV system called the Optical parametric oscillator.

1.1.2 The Optical Parametric Oscillator

The Optical Parametric oscillator (OPO) is an alternative tool for non-linear generation of entangled photons where a pump photon (ω_p) is converted into two lower energy beams, known as the signal photon (ω_s) and the idler photon (ω_i) occurring due to excitation of a nonlinear crystal when struck by an external electromotive force, as shown in Fig (1). Nonlinear crystal is media in which dielectric polarization responds nonlinearity to the electric field of light.

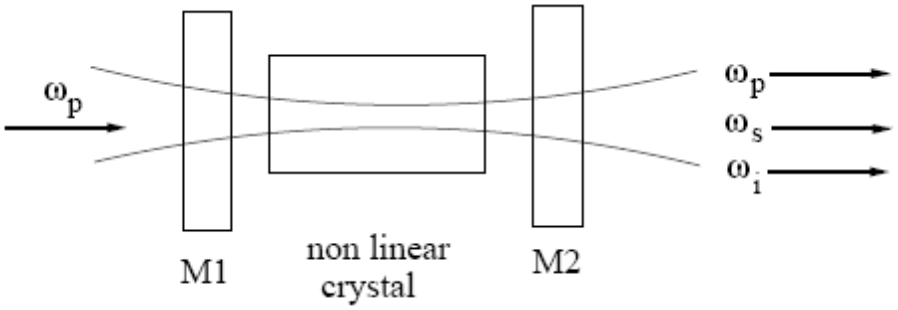

Figure (1): Optical parametric oscillator; the mirror M1 is highly reflective for the signal wave (ω_s) or/and idler wave (ω_i), highly transparent for the pump wave (ω_p). The output coupler M2 is partially reflecting ω_s or/and ω_i and highly transparent for ω_p (Bass, 2001).

The total energy of the two photons produced from the parametric non-linear interaction is equal to the energy of the photon originally fired from the laser. The photon energy and momentum are conserved according to

$$\omega_p = \omega_s + \omega_i \qquad (1.4a)$$

$$k_p = k_s + k_i \qquad (1.4b)$$

where ω_p, ω_s, ω_i and k_p, k_s, k_i are the photon angular frequency and kinetic energy for the pump (p), signal (s) and idler (i) photons respectively. The model Hamiltonian for the OPO is

$$\hat{\mathrm{H}} = \hbar\left(\omega_a \hat{a}^\dagger \hat{a} + \omega_b \hat{b}^\dagger \hat{b} + \alpha(t)\, \hat{a}^\dagger \hat{b} + \alpha^*(t) \hat{b}^\dagger \hat{a}\ \right) \qquad (1.5)$$

where $\hat{a}(\hat{a}^\dagger)$ and $\hat{b}(\hat{b}^\dagger)$ are the signal and idler annihilation (creation) operators, ω_a, ω_b and ω_p are the signal, idler and pump frequencies respectively and $\alpha(t)$ is a time-dependent interaction parameter which describes an external classical pump field. The zero-point energy components have been dropped in equation (1.5) since these components generally lead to global phase

factors only. The system represented by (1.5) is a two-particle system where the signal photon is denoted by mode ‘a’ and the idler photon is denoted by mode ‘b’. The signal photon is taken to be initially in the horizontal polarization state and the idler photon is taken to be initially in the vertical polarization state. The signal and idler photons can be in either horizontal or vertical polarization states at any initial time t=0. The OPO is a CV system that has been tested for production of quantum dynamics and entanglement.

1.1.3 The quantum dynamics and entanglement in the OPO

Quantum systems evolve with time and produce wave functions which can be solved within the Schrödinger, Heisenberg's or Dirac (or, interaction) pictures of quantum mechanics. The study of quantum dynamics in the OPO and non-degenerate parametric down conversion (NPDC) has been widely studied where time evolution equations are solved (Rekdal and Skagerstam, 1999; Akeyo, 2008). In a NPDC, the Lie algebraic method was applied to solve equation for time evolution operator within the interaction picture using Schrödinger equation in a process involving complications of operator expansion theorems under a parametric resonance (Rekdal and Skagerstam, 1999). In the Schrödinger picture, the operators are fixed while the Schrödinger equation changes the basis with time. A more simplified matrix method was later used to solve time evolution equations arising from NPDC within the Heisenberg picture to produce much simpler solutions of time evolution operator (Akeyo, 2008). In the Heisenberg picture, it is the operators which change in time while the basis of the space remains fixed making the system more mathematically pleasing. In the Dirac picture, both the basis and the operators carry time-dependence. The quantum dynamics of two degenerate optical parametric oscillators with mutual injections was analytically and numerically studied (Kenta and Yoshihisa, 2015). The cavity mode in the optical coupling path between the two oscillator facets was explicitly considered. In this case, stochastic equations for the oscillators and mutual injection path based on the positive *P* representation were derived. Studies on non-degenerate optical parametric oscillator with injected signal (INOPO) were carried out using a Heisenberg picture Hamiltonian (Coutinho and Santos, 2005). Although exact Heisenberg equations of motion were found from this Hamiltonian, it was, at the very least, extremely difficult to solve nonlinear operator equations hence making it difficult to obtain simple and exact solutions of time evolution operator.

Heisenberg's equations and matrix method are preferred because they provide simple and exact solutions of time evolution equations (Akeyo, 2008). A part from production of the quantum dynamical properties, the OPO is a system with potential for generation of entangled photons.

Continuous variable entanglement was demonstrated for the first time in the OPO operating below threshold in 1990. Entanglement in the above-threshold OPO remained an experimental challenge until 2005, when it was first observed (Villar and Cassemiro, 2005). Entanglement features for a full quantum treatment of OPO has been studied where time evolution equations are solved through writing of the density operator equation in the Wigner representation using equivalent Langevin equations to obtain analytical results (Villar and Cassemiro, 2006). Multipartite entanglement (entanglement of more than two particles) was generated on a massive scale in the spectrum, or optical frequency comb, of a single optical parametric oscillator (OPO) emitting well above threshold (Shahrokhshahi and Pfister, 2012). The multipartite nature of entanglement was verified by evaluating the van Loock-Furusawa criterion for a particular set of entanglement witnesses deduced from physical considerations. A two-color entanglement was observed measured in the above-threshold OPO (Su and Tan, 2006). The entanglement features described above were limited to above-threshold and below-threshold OPO and were not carried out under all conditions of interaction in explicit solutions of time evolution equations.

The conditions under which a multi-mode nano-mechanical resonator can be driven into highly non-classical states, operating as a purely mechanical parametric oscillator was investigated theoretically (Johansson, 2014). The quantum entangled states of the system violate Bell inequalities with homodyne quadrature measurements. The parameter regimes were analyzed for such Bell inequality violations, and while experimentally challenging, it was believed that the realization of such states lies within reach. Several interesting aspects of a new light source, two-level atom inside an Optical Parametric Oscillator was considered where a Bell state for atom and field was presented as (Rice, 2005)

$$|\psi\rangle = \frac{1}{\sqrt{2}}(|0, e\rangle - |1, g\rangle) \qquad (1.6)$$

where the Bell basis state $|e\rangle$ is in excited state corresponding to the horizontal polarization and $|g\rangle$ is in ground state corresponding to the vertical polarization. The dynamics of the quantum Rabi model was analyzed for two qubits interacting through a common bosonic field mode (resonator), focusing on the generation and detection of maximally entangled Bell states (Matteo, 2014). The Bell state (1.6) for the atom-field interaction was presented in a general and simple form which does not evolve with time for determination of entanglement in the OPO.

The CHSH (Clauser-Horne-Shimony-Holt) Bell inequality is an entanglement criterion commonly used for test of entanglement of polarization states and was convincingly tested for the first time in 1982, following the introduction of Bell states in 1962. Entanglement is exhibited by violations of the CHSH Bell inequality. The evolution of a bipartite entangled quasi-bell state in a strongly coupled qubit oscillator system in the presence of a static bias was studied, and extended to the ultra-strong coupling regime (Chakrabarti and Jenisha, 2015). Adiabatic approximation was used to obtain reduced density matrix of the qubit for the strong coupling domain in closed form involving linear combinations of the Jacobi theta functions. To obtain measures of entanglement and the mixedness of the bipartite system the von Neumann entropy of the reduced density matrix of the qubit was considered. Apart from employing the adiabatic approximation no other simplification has been made for deriving the reduced density matrix elements. A test of Bell inequality using polarization entangled photons from a Spontaneous Parametric down Conversion (SPDC) has shown a violation of Bell's inequality (Eberhard, 1999). This study will consider the possibility of producing a violation of Bell's inequality using entangled photons from a semi-classical OPO through construction of explicit solutions of reduced density matrix elements.

We observe that the OPO has been studied below-threshold and above threshold using Bell state vectors which do not vary with time hence entanglement produced is not dynamic. Expressing

Heisenberg's equations into matrix form provides the required exact solutions of time evolution equations which are appropriate for study of entanglement properties of photon polarization state vectors. The study of entanglement in the OPO has not been exploited fully especially using exact solutions of time evolving polarization states and time evolving Bell state vectors under all conditions of interaction. We therefore study the dynamical evolution of entanglement in the semi-classical OPO using exact solutions of Heisenberg's equations to obtain results through application of explicit solutions of Bell state vectors under all conditions of interaction.

1.2 Statement of the Problem

Many advances have been made in the rapidly expanding research area of quantum entanglement since the year 1935, especially with discrete variable states under resonance. Nevertheless, in quantum optics, there are a number of quantum systems that must be described by continuous variable states. One such important continuous variable system which has not received much attention analytically, in particular within the framework of polarization state dynamics is the OPO. We demonstrate the dynamical evolution of continuous variable entanglement in a semi-classical OPO using general time evolving polarization state vectors arising from exact analytical solutions of Heisenberg's equations of the system through violation of Bell inequalities, under all conditions of interaction with frequency detuning.

1.3 Objectives of the Study

The objectives of the study are:

1. To obtain exact solutions of Heisenberg's equations to determine the time evolution operator and time evolving polarization state vectors of signal and idler photons in a semi-classical OPO.
2. To construct Bell state vectors using the general time evolving polarization state vectors of signal and idler photons in the semi-classical OPO.
3. To test entanglement of polarization states of the signal-idler photon pair in the semi-classical OPO, under all conditions of interaction.

1.4 Significance of the study

Quantum entanglement is a fundamental quantum mechanical phenomenon with great potential for practical applications in fields of quantum computation and quantum information processing. We provide an appropriate and elaborate way of displaying entanglement in the semi-classical OPO and this widens the scope for implementation of various quantum communication protocols such as quantum teleportation, quantum key distribution, and dense coding (increased communication channel capacity). The photon polarization states are used because they produce larger Hilbert space for higher bandwidth in quantum communication than the spin states. The semi-classical mode is used for entanglement in the OPO to obtain entanglement properties due to a quantized electromotive field driven by a classical external field. The entanglement of photon polarization states in a semi-classical OPO promotes the development of quantum technology whereby the entangled photon polarization states provide useful quantum mechanical properties which can be used in quantum computing and other quantum communication protocols.

CHAPTER TWO: LITERATURE REVIEW

2.1 Entanglement properties of OPO

The Optical parametric oscillator (OPO) has been studied since the 1960's (Kingston, 1962) and was used to generate squeezed coherent states and entangled states of light (Giordmaine and Miller, 1965). In the early 1990's, continuous variable (CV) entanglement was demonstrated for the first time in an OPO, where below-threshold (Pereira and Kimble, 1992) operation was considered. Entanglement in the above-threshold OPO, on the other hand, remained an experimental challenge until 2005, when it was first observed (Villar and Cassemiro, 2005), and subsequently by two other groups (Su and Tan, 2006). Correlations in the non-degenerate optical parametric oscillator (NOPO) were investigated both above and below threshold (Reid and Drummond, 1989). The effects of phase diffusion in the signal and idler modes were studied in the above-threshold case, beginning with the positive P-representation equations of motion for the interacting fields. The quantum dynamics of two degenerate optical parametric oscillators with mutual injections were analytically and numerically studied (Kenta and Yoshihisa, 2015). The cavity mode in the optical coupling path between the two oscillator facets was explicitly considered. In this case, stochastic equations for the oscillators and mutual injection path based on the positive *P* representation were derived. The systems of two gradually pumped oscillators with out-of-phase mutual injections were simulated, and their quantum states investigated. When the incoherent loss of the oscillators other than the mutual injections is small, the squeezed quadratic amplitudes $\hat{p}$ in the oscillators are positively correlated near the oscillation threshold. It indicates finite quantum correlation, and entanglement between the intra-cavity sub-harmonic fields. The entanglement was limited to OPO operating below-threshold and above-threshold and was not considered under all conditions of interaction.

Studies on non-degenerate optical parametric oscillator with injected signal (INOPO) were carried out using a Heisenberg picture Hamiltonian of the form (Coutinho and Santos, 2005)

$$\hat{\mathrm{H}} = \sum_{i=0}^{2} \hbar\omega_i \hat{a}_i{}^{\dagger}\hat{a}_i + i\hbar\chi(\hat{a}_1{}^{\dagger}\hat{a}_2{}^{\dagger}\hat{a}_0 - \hat{a}_1\hat{a}_2\hat{a}_0{}^{\dagger}) + i\hbar(\varepsilon_0 e^{-\omega_0 t}\hat{a}_0{}^{\dagger} - \varepsilon_0{}^{*} e^{i\omega_0 t}\hat{a}_0)$$

$$+ i\hbar(\varepsilon_1 e^{-i\omega_1 t}\hat{a}_1{}^{\dagger} - \varepsilon_1{}^{*} e^{i\omega_1 t}\hat{a}_1) + \sum_{i=0}^{2}(\hat{a}_i\hat{\Gamma}_i{}^{\dagger} + \hat{a}_i{}^{\dagger}\hat{\Gamma}_i) \qquad (2.0)$$

where a strong external driving field for the pump field, ε_0, was considered at frequency ω_0, and a generally much weaker injected field for the signal field, ε_1, at frequency ω_1. Each field is damped via the cavity output mirror, interacting with the reservoir fields, denoted by the bath operators $\hat{\Gamma}_j$. The effective second-order nonlinearity of the crystal is represented by the constant χ. Quantum entanglement was demonstrated by the INOPO model system using the Einstein-Podolsky-Rosen (EPR) paradox under reasonably low levels of injected signal. In contrast to the normal optical parametric oscillator operating below threshold, these features are demonstrated with relatively intense fields. Although exact Heisenberg equations of motion can be found from this Hamiltonian, it was extremely difficult to solve nonlinear operator equations hence making it difficult to obtain simple and exact solutions of time evolution operator.

Two-color entanglement was observed measured in the above-threshold OPO (Su and Tan, 2006). The difference between their setup and others is lower cavity finesse for the pump field. For a lower finesse, phase shifts accumulated inside the cavity should be smaller; hence the excess noise generated should also be smaller. This became the first system proposed to observe continuous variable entanglement. A theoretical and experimental treatment of phase noise and entanglement in the above-threshold OPO was presented using a linearized model of OPO for prediction of a short noise limited pump beam (Villar and Cassemiro, 2006). The model includes losses and also allows for non-vanishing detuning of pump, signal, and idler modes with respect to the OPO cavity. The equations describing the evolution of signal, idler, and pump amplitudes, inside the triply resonant OPO cavity were obtained by writing the density operator equation of motion in the Wigner representation, and then searching for a set of equivalent Langevin equations.

$$\tau \frac{d}{dt}\alpha_o = -\gamma^1{}_o(1 - i\Delta_o)\alpha_o - 2\chi^*\alpha_1\alpha_2 + \sqrt{2\gamma_o}\alpha_o{}^{in} + \sqrt{2\mu_o}\delta\upsilon_o \qquad (2.1a)$$

$$\tau \frac{d}{dt}\alpha_1 = -\gamma^1(1 - i\Delta)\alpha_1 + 2\chi\alpha_o\alpha^*{}_2 + \sqrt{2\gamma}\delta u_1 + \sqrt{2\mu}\delta\upsilon_1 \qquad (2.1b)$$

$$\tau \frac{d}{dt}\alpha_2 = -\gamma^1(1 - i\Delta)\alpha_2 + 2\chi\alpha_o\alpha^*{}_1 + \sqrt{2\gamma}\delta u_2 + \sqrt{2\mu}\delta\upsilon_2, \qquad (2.1c)$$

where γ and γ_o are half the transmissions of the mirrors, γ^1 and $\gamma_o{}^1$ are the total intracavity losses, $\mu = \gamma^1 - \gamma$ and $\mu_o = \gamma_o{}^1 - \gamma_o$ are the spurious intracavity losses, Δ and Δ_o are the detuning's of the OPO cavity relative to the fields central frequencies, and τ is the cavity roundtrip time. A full quantum treatment was then performed, neglecting losses and for zero detuning. Excess noise in the phase sum of the twin beams was measured as a function of pump power relative to threshold and it was found that it decreases as pump power is lowered. It was discovered that excess pump noise is generated inside the OPO cavity containing the nonlinear crystal. This study involved the use of a set of equivalent Langevin equations for determination of solutions of time evolution equations to obtain entanglement in the OPO limited to above-threshold and full quantum treatment.

2.2 Multipartite entanglement in the OPO

It was showed that multipartite entanglement is generated on a massive scale in the spectrum, or optical frequency comb, of a single optical parametric oscillator (OPO) emitting well above threshold (Shahrokhshahi and Pfister, 2012). The simplest possible case of an OPO with a single, non-degenerate nonlinear interaction was considered having an interaction-picture Hamiltonian

$$\hat{\mathrm{H}}_{\mathrm{int}} = 2i\hbar\chi\beta\sum_{i=1}^{n}(pa_i{}^{\dagger}a_{-i}{}^{\dagger} - p^{\dagger}a_i a_{-i}) \qquad (2.2)$$

where p is the annihilation operator of the pump field, β is the classical (real) and constant (un-depleted) pump field and $a_{\pm i}$ are the photon annihilation operators of entangled Q modes $\pm i$. Above the OPO threshold, the un-depleted classical pump approximation can still be taken to hold and the generation of EPR states has also been shown to be possible just as shown earlier theoretically (Reid and Drummond, 1989) and experimentally (Villar and Cassemiro, 2005). However, the un-depleted classical pump approximation breaks down if the external pump power is increased significantly above threshold. The quantum dynamics of the strongly depleted pump field are responsible for the onset of the entanglement by correlating the two-mode squeezed, bipartite-entangled pairs of OPO signal fields. The multipartite nature of entanglement was verified by evaluating the van Loock-Furusawa criterion for a particular set of entanglement witnesses deduced from physical considerations. It was shown that a single OPO operating well above threshold can generate multipartite entanglement in its quantum optical frequency comb. Above the OPO threshold, the un-depleted classical pump approximation was taken to hold for determination of multipartite entanglement. The mulpartite entanglement was limited to the OPO system operating well above threshold at quantum optical frequency comb and not under all conditions of interaction.

2.3 Bell inequalities and entanglement in the OPO

The conditions under which a multi-mode nano-mechanical resonator can be driven into highly non-classical states, operating as a purely mechanical parametric oscillator were investigated theoretically (Johansson, 2014). In the original frame, the Hamiltonian with a rotating-wave approximation was used of the form

$$\hat{\mathrm{H}} = \sum_{k=0}^{2} \omega_k a_k{}^{\dagger} a_k + ik(a_1{}^{\dagger} a_2{}^{\dagger} a_0 - a_1 a_2 a_0{}^{\dagger}) \qquad (2.3)$$

where $\hat{a}_1$ and $\hat{a}_2$ are the signal and idler modes, respectively, and $\hat{a}_0$ is the pump mode. It was found that when the device is cooled to near its ground state, and certain mode matching conditions are satisfied, it is possible to prepare distinct resonator modes in quantum entangled

states that violate Bell inequalities with homodyne quadrature measurements. The parameter regimes are analyzed for such Bell inequality violations, and while experimentally challenging, it was believed that the realization of such states lies within reach. This is a re-imagining of a quintessential quantum optics experiment by using phonons that represent tangible mechanical vibrations. The results demonstrate that while realistically it will not be possible to violate any Bell inequality in the steady state, there can be a significant duration of time in which the transient evolution from the ground state (prepared by cooling) to the steady state where the state of the system violates Bell inequalities. This system operates as a purely mechanical parametric oscillator and projects that there is a significant duration of time for violation of Bell inequalities of entangled states. In the current work we test explicitly the violation of Bell inequalities at any given time by use of entangled polarization states arising from the semi-classical OPO under all conditions of interaction.

Several interesting aspects of a new light source, two-level atom or N two-level atoms were considered inside an Optical Parametric Oscillator (Rice, 2005). The atom and optical cavity were assumed to be resonant at ω and the system driven by light at 2ω. A conditioned wave function type of system was considered, which evolves via a non-Hermitian Hamiltonian, and associated collapse processes.

$$\left|\psi_C(t)\right\rangle = \sum_{n=0}^{\infty} C_{g,n}(t)e^{-iE_{g,n}t}\left|g,n\right\rangle + C_{e,n}(t)e^{-iE_{e,n}t}\left|e,n\right\rangle \qquad (2.4a)$$

$$\hat{\mathrm{H}} = -ika^{\dagger}a - i\frac{\gamma}{2}\sigma_{+}\sigma_{-} + i\hbar F(a^{\dagger 2} - a^{2}) + i\hbar G(a^{\dagger}\sigma_{-} - a\sigma_{+}) \qquad (2.4b)$$

The Hamiltonian (2.4b) represents Jaynes-Cummings model of a two-level atom-field interaction for degenerate parametric amplification process where we also have collapse operator $C = \sqrt{ka}$ representing cavity loss. The usual Jaynes-Cummings atom-field coupling in the rotating wave and dipole approximations is

$$\alpha = \mu(\omega_0 / \hbar\varepsilon_0 V)^{1/2} \qquad (2.5)$$

The cavity-mode volume is V, and the atomic dipole matrix element is μ connecting the ground, g, and excited, e, states. The effective two-photon driving field F is proportional to the intensity $I_{in}(2\omega_0)$ of a driving field at twice the resonant frequency of the atom. γ is the spontaneous emission rate directed out from the sides of the cavity, and k is the rate of intra-cavity intensity decay. For $g = k$ and $\gamma = 0.0$, a Bell state was obtained of the form in (1.6) for the atom and field. Interesting entangled states were generated upon detection of a transmitted photon. The generated state will change with time, and eventually disappear, but is prepared with high fidelity in a probabilistic manner. Coupling such systems together as in previous schemes allows one to generate a larger variety of entangled states; this method can be used to entangle systems spatially separated, and can be used in teleportation and dense coding protocols. The Bell state (1.6) for the atom-field interaction is presented in a simple form which does not evolve with time hence not good for demonstration of dynamical evolution of entanglement.

The dynamics of the quantum Rabi model for two qubits interacting through a common bosonic field mode (resonator) were analyzed, focusing on the generation and detection of maximally entangled Bell states (Matteo, 2014). Two qubits were considered of transition frequencies ω_i between the states $|e\rangle_i$ and $|g\rangle_i$,i=1, 2, interacting with a common bosonic field mode, oscillating at the frequency ω and described by the field operators $\hat{a}$ and $\hat{a}^\dagger$. The system was described by the quantum Rabi model with Hamiltonian given by

$$\hat{H} = \hbar\omega a^\dagger a + \hbar \sum_{i=1,2} \frac{\omega_i}{2} \sigma_z{}^{(i)} + \hbar \sum_{i=1,2} \Gamma_i \sigma_x{}^{(i)} (a^\dagger + a) \qquad (2.6)$$

where Γ_1 and Γ_2 are the coupling constants and

$$\sigma_z{}^{(i)} = |e\rangle_i\langle e| - |g\rangle_i\langle g| \qquad (2.7a)$$

$$\sigma_x^{(i)} = \sigma_+^{(i)} + \sigma_-^{(i)}, \tag{2.7b}$$

The raising and lowering operators are

$$\sigma_+^{(i)} = |e\rangle_i\langle g| \tag{2.8a}$$

$$\sigma_-^{(i)} = |g\rangle_i\langle e| \tag{2.8b}$$

respectively, of the i-th qubit. The Bell states were introduced as

$$\left|\psi_{(\pm)}\right\rangle = \frac{1}{\sqrt{2}}(|gg\rangle \pm i|ee\rangle, \qquad \left|\phi_{\pm}\right\rangle = \frac{1}{\sqrt{2}}(|eg\rangle \pm i|ge\rangle) \tag{2.9}$$

Analytical results for the unitary dynamics of this system in the slow-qubit (or degenerate) regime were obtained, considering ultra-strong coupling between qubits and resonator mode, for which the rotating wave approximation is no longer applicable. The dynamics beyond the slow-qubit condition were also numerically investigated in order to study the validity of the model in the presence of less strict conditions. The physical dynamics of the system captured by the slow-qubit approximation in the deep strong coupling regime is radically different from a Jaynes-Cummings-like dynamics, as it involves multi-photon processes and in principle spans the entire Fock space of the resonator mode. The oscillatory behavior of the dynamics generates maximally entangled Bell states, depending on a precise relation between the coupling constants. The range of validity of this approximation was explored by means of numerical integration of the Schrödinger equation ruled by the whole quantum Rabi Hamiltonian; the study at which extent the qubit frequencies can be increased to obtain a high-fidelity generation of Bell states. The Bell states obtained in (2.9) are presented in simple form that does not vary with time hence not good study of the dynamical evolution of entanglement.

Entangled states are very interesting states because they exhibit correlations that have no classical analog. The discussion between EPR and e.g. Niels Bohr was considered a merely philosophical one until in 1964 when John Bell suggested to measure certain correlations between entangled entities. When only classical correlations existed then

$$|S| \leq 2 \qquad (2.10)$$

where S is a numerical measurement arising from entanglement criteria. The correlations would violate an inequality (Bell's inequality) if quantum mechanics was correct. Measurement bases are chosen such that a maximal violation of equation (2.10) is obtained as

$$|S| = 2\sqrt{2} \qquad (2.11)$$

A quite number of experimental tests of Bell inequality using polarization entangled photons from a spontaneous parametric down conversion source have been done. Bell inequalities were used for test of entanglement using polarization entangled photons from a Spontaneous Parametric down Conversion (SPDC) which showed a violation of Bell's inequality (Eberhard, 1999). In 1994 it was discovered that not all entangled states violate a Bell inequality (Popescu, 1994). It was also shown that the Werner state, a mixture of the maximally entangled state and the maximally mixed state can be entangled (inseparable) and yet not violate the convectional Bell inequality (Munro, Nemote and White, 2001). Despite the fact that the possibility of quantum entanglement was acknowledged almost as soon as quantum theory was discovered, it is only in recent years that consideration has been given to finding methods to quantify it (Munro, Nemote and White, 2001). In the current study we obtain the strength of entanglement through violation of Bell inequalities in the OPO for the purpose of quantifying the entanglement produced.

The evolution of a bipartite entangled quasi-bell state was studied in a strongly coupled qubit oscillator system in the presence of a static bias, and was extended to the ultra-strong coupling regime (Chakrabarti and Jenisha, 2015). The adiabatic approximation was used to obtain reduced density matrix of the qubit for the strong coupling domain in closed form involving linear combinations of the Jacobi theta functions. Starting with a quasi-Bell bipartite initial state the

evolution of the reduced density matrices of the qubit and oscillator was obtained, respectively. The adiabatic approximation in quantum mechanics is a method by which approximate solutions to time dependent Schrodinger equation can be found. In this study the time dependence of quasi-Bell states was analytically studied in a coupled qubit-oscillator system within the adiabatic approximation scheme using a Hamiltonian that reads in natural units $\hbar = 1$

$$\hat{\mathrm{H}} = -\frac{\Delta}{2}\sigma_x - \frac{\varepsilon}{2}\sigma_z + \omega a^{\dagger}a + \lambda\sigma_z(a^{\dagger} + a) \qquad (2.12)$$

where the harmonic oscillator with a frequency ω is described by the raising and lowering operators $(a^{\dagger}, a \,|\, \hat{n} \equiv a^{\dagger}a)$, and the qubit characterized by an energy splitting Δ as well as an external static bias ε was expressed via the spin variables (σ_x, σ_z). The qubit-oscillator coupling strength is denoted by λ. The reduced density matrix of the oscillator yields the phase space Husimi Q-distribution. In the strong coupling regime, the Q-function evolves to uniformly separated macroscopically distinct Gaussian peaks representing 'kitten' states at certain specified times that depend on multiple time scales present in the interacting system. For the ultra-strong coupling realm the delocalization in the phase space of the oscillator was studied by using the Wehrl entropy. For a small phase space amplitude the entangled Quasi-Bell state develops during its time evolution, squeezing property and non-classicality of the photon statistics are measured by the quadrature variance and the Mandel parameter, respectively. To obtain measures of the entanglement and the mixedness of the bipartite system the von Neumann entropy of the reduced density matrix of the qubit was considered. Apart from employing the adiabatic approximation no other simplification has been made for deriving the reduced density matrix elements. In the current study we derive reduced density matrix elements for the OPO within the platform of polarization state dynamics.

2.4 Quantum dynamics and entanglement in the OPO

In quantum optics, a two-mode Hamiltonian model of a parametric down-conversion process has been widely studied particularly under resonance where time evolution equations are solved (Rekdal and Skagerstam, 1999; Akeyo, 2008). A general non-resonant two-mode parametric

down-conversion process was studied in detail considering coupled harmonic oscillators described by a two-mode Hamiltonian (Rekdal and Skagerstam, 1999)

$$\hat{\mathrm{H}} = \hbar\omega_a\left(\hat{a}^\dagger\hat{a} + \frac{1}{2}\right) + \hbar\omega_b\left(\hat{b}^\dagger\hat{b} + \frac{1}{2}\right) + i\hbar\left(g(t)\hat{a}\hat{b} - g^*(t)\hat{a}^\dagger\hat{b}^\dagger\right) \quad , \quad (2.13)$$

where $(\hat{a}, \hat{a}^\dagger)$ and $(\hat{b}, \hat{b}^\dagger)$ are the annihilation and creation operators of the oscillators, while g(t) is a time-dependent coupling parameter which describes an arbitrary classical pump field due to interaction between the signal mode '*a'* and idler mode '*b'*. The Hamiltonian (2.13) applies to a parametric down conversion process while the Hamiltonian (1.5) of the current study applies to an OPO. The Lie algebraic method was applied to solve the equation for time evolution operator within the interaction picture for non-degenerate parametric down conversion (NPDC) by defining

$$g(t) \equiv g(t)e^{-i(\omega_a + \omega_b)t} \quad (2.14)$$

and using the corresponding Schrödinger equation

$$i\frac{d}{dt}U(t) = i[g(t)e^{-i(\omega_a+\omega_b)t} - g^*(t)e^{i(\omega_a+\omega_b)t}]U(t) \quad , \quad (2.15)$$

where U(t) is the time evolution operator which brings about change of state due to passage of time.

Due to the presence of the Lie-algebra of SU (1;1) the Wei-Norman technique was employed in a process involving complications of operator expansion theorems to obtain analytical expression for time-evolution operator

$$U(t) = e^{A_+(t)K_+}e^{2A_0(t)K_0}e^{A_-(t)K_-} \quad , \quad (2.16a)$$

where

$$K_{-} \equiv \hat{a}\hat{b},\ K_{+} \equiv \hat{a}^{\dagger}\hat{b}^{\dagger},\ K_{0} \equiv \frac{\hat{a}^{\dagger}\hat{a}+\hat{b}\hat{b}^{\dagger}}{2} \qquad (2.16b)$$

The quantum dynamics of a two-mode non-resonant parametric down-conversion process was studied by recasting the time evolution equations for the basic operators in an equivalent spin equation form with simpler exact solutions for a pump field with harmonic time dependence (Akeyo, 2008). A simpler matrix-based method of solution was developed for the study whereby time evolution equations were determined directly through Heisenberg's equation to obtain exact and explicit solution of time evolution operator

$$U(t) = \begin{pmatrix} \mu(t)e^{-\frac{i}{2}(\Omega+2\omega_a)t} & \nu(t)e^{-\frac{i}{2}(\Omega+2\omega_a)t} \\ \nu(t)e^{\frac{i}{2}(\Omega+2\omega_a)t} & \mu^{*}(t)e^{\frac{i}{2}(\Omega+2\omega_a)t} \end{pmatrix}, \qquad (2.17)$$

where

$$\omega+\Delta = \Omega+2\omega_a\ ;\quad \omega-\Delta = \Omega+2\omega_b\ ;\quad \beta = \pm g\sqrt{1-k^2}\ ;\ k = \tfrac{\Omega}{2g} \qquad (2.18a)$$

$$\omega = \omega_a+\omega_b,\ \Omega = 0,\ k = 0,\ \beta = g \qquad (2.18b)$$

Exact and simpler solutions of time evolution equations were obtained easily using Heisenberg's equations of motion expressed in matrix form rather than in Schrödinger picture using the Lie algebraic method. The results obtained in (2.16a) and (2.17) for time evolution operators were limited to the study of dynamical quantum features of a parametric down conversion process. The quantum entanglement features related to the system were not studied. We therefore present the OPO not only as a system for production of quantum dynamics but also as a tool for study of entanglement features.

We observe that, in general, the dynamical features of a two-level atom interacting with a classical electromagnetic field are the same as the dynamical features of a semi-classical OPO described in terms of signal-idler photon polarization states. On the other hand, the dynamical features of a Jaynes-Cummings interaction between a two-level atom and a quantized electromagnetic field are the same as the dynamical features of a fully quantized parametric oscillation process described in terms of the signal-idler photon polarization states (Akeyo, 2013). The parametric down conversion process has received much attention in terms of determination of quantum dynamical features of a two-mode Hamiltonian (2.13) where time evolution equations were solved. Exact and simpler solutions of time evolution equations were obtained easily using Heisenberg's equations of motion expressed in matrix form rather than the Schrödinger equation using the Lie algebraic method. In this work, apart from the study of quantum dynamics, we study quantum entanglement in the OPO. The study is based on determination of entanglement features within the framework of polarization state dynamics. Entanglement presented in the OPO was demonstrated using Bell states that do not vary with time, limited to above and below threshold conditions hence could not produce fully the required dynamics of quantum entanglement. In the present work, we determine exact and simpler solutions of time evolution equations obtained easily using Heisenberg's equations of motion, under all conditions of interaction for the pump field. We obtain explicitly the solutions of time evolving bell state vectors and reduced density matrices for use in violation of Bell inequalities. Expressing Heisenberg's equations into matrix form provides the required exact solutions of time evolution equations which are appropriate for study of entanglement features of photon polarization state vectors arising from the semi-classical OPO.

CHAPTER THREE: MATERIALS AND METHODS

3.1 Heisenberg's equations and matrix method

We consider a model of semi-classical parametric oscillation process described by a two-mode Hamiltonian (1.5). The dynamics generated by (1.5) is described through Heisenberg's equations

$$i\hbar\frac{d\hat{a}}{dt}=\left[\hat{a},\hat{\mathrm{H}}\right]=\frac{\partial\hat{\mathrm{H}}}{\partial\hat{a}^{\dagger}}=\hbar\left(\omega_a\hat{a}+\alpha(t)\hat{b}\right) \qquad (3.0a)$$

$$i\hbar\frac{d\hat{b}}{dt}=\left[\hat{b},\hat{\mathrm{H}}\right]=\frac{\partial\hat{\mathrm{H}}}{\partial\hat{b}^{\dagger}}=\hbar\left(\alpha^{*}(t)\hat{a}+\omega_b\hat{b}\right) \qquad (3.0b)$$

for annihilation operators $\hat{a},\hat{b}$ of the signal and idler photons respectively. The signal photon is represented by mode 'a' and is initially in the horizontal polarization state. The idler photon is represented by mode 'b' and is initially in the vertical polarization state.

The signal photon and idler photon can be taken to be in either horizontal or vertical polarization states at initial time t=0.

The time evolution equations (3.0a) and (3.0b) can be rewritten as

$$i\hbar\frac{d}{dt}\begin{pmatrix}\hat{a}\\ \hat{b}\end{pmatrix}=\hbar\begin{pmatrix}\omega_a & \alpha(t)\\ \alpha^{*}(t) & \omega_b\end{pmatrix}\begin{pmatrix}\hat{a}\\ \hat{b}\end{pmatrix} \qquad (3.1)$$

Alternatively, taking the signal photon represented by mode 'a' to be initially in the vertical polarization state and the idler photon represented by mode 'b' to be initially in the horizontal polarization state, we obtain an equivalent form of (3.1)

$$i\hbar\frac{d}{dt}\begin{pmatrix}\hat{b}\\ \hat{a}\end{pmatrix}=\hbar\begin{pmatrix}\omega_b & \alpha^{*}(t)\\ \alpha(t) & \omega_a\end{pmatrix}\begin{pmatrix}\hat{b}\\ \hat{a}\end{pmatrix} \qquad (3.2)$$

We identify in (3.1) and (3.2) two-component photon pair polarization operator vectors which are alternate to each other in the form

$$\hat{A} = \begin{pmatrix} \hat{a} \\ \hat{b} \end{pmatrix} = \hat{a}|0\rangle + \hat{b}|1\rangle = \hat{a}|H\rangle + \hat{b}|V\rangle \qquad (3.3a)$$

$$\hat{B} = \begin{pmatrix} \hat{b} \\ \hat{a} \end{pmatrix} = \hat{b}|0\rangle + \hat{a}|1\rangle = \hat{b}|H\rangle + \hat{a}|V\rangle \qquad (3.3b)$$

where the photon horizontal and vertical polarization state vectors $|H\rangle$ and $|V\rangle$ are defined in (1.2a) and (1.2b).

We identify in (3.1) and (3.2) time evolution Hamiltonian matrices known as generators in the form

$$\hat{\mathrm{H}}^{I}{}_{A} = \hbar \begin{pmatrix} \omega_a & \alpha(t) \\ \alpha^*(t) & \omega_b \end{pmatrix} \qquad (3.4a)$$

$$\hat{\mathrm{H}}^{I}{}_{B} = \hbar \begin{pmatrix} \omega_b & \alpha^*(t) \\ \alpha(t) & \omega_a \end{pmatrix} \qquad (3.4b)$$

Equations (3.1) and (3.2) becomes

$$i\hbar \frac{d\hat{A}}{dt} = \hat{\mathrm{H}}^{I}{}_{A}\hat{A} \qquad (3.5a)$$

$$i\hbar \frac{d\hat{B}}{dt} = \hat{\mathrm{H}}^{I}{}_{B}\hat{B} \qquad (3.5b)$$

We introduce the usual Pauli spin operators

$$\mathrm{I} = \begin{pmatrix} 1 & 0 \\ 0 & 1 \end{pmatrix}, \qquad \sigma_x = \begin{pmatrix} 0 & 1 \\ 1 & 0 \end{pmatrix} \quad , \quad \sigma_y = \begin{pmatrix} 0 & -i \\ i & 0 \end{pmatrix} \quad , \quad \sigma_z = \begin{pmatrix} 1 & 0 \\ 0 & -1 \end{pmatrix} \qquad (3.6a)$$

$$\hat{S}_0 = \frac{1}{2}\mathrm{I} \quad , \quad \hat{S}_x = \frac{1}{2}\sigma_x \quad , \quad \hat{S}_y = \frac{1}{2}\sigma_y \quad , \quad \hat{S}_z = \frac{1}{2}\sigma_z \qquad (3.6b)$$

$$\hat{S}_+ = \frac{1}{2}\left(\sigma_x + i\sigma_y\right) = \begin{pmatrix} 0 & 1 \\ 0 & 0 \end{pmatrix} \quad , \quad \hat{S}_- = \frac{1}{2}\left(\sigma_x - i\sigma_y\right) = \begin{pmatrix} 0 & 0 \\ 1 & 0 \end{pmatrix} \qquad (3.6c)$$

$$\hat{S}_x = \frac{1}{2}\left(\hat{S}_+ + \hat{S}_-\right) \qquad (3.6d)$$

We use spin operators (3.6a-d) to express (3.4a) and (3.4b) in the form

$$\hat{\mathrm{H}}^I{}_A = \hbar\left(\Omega_{ab}\hat{S}_0 + \omega_{ab}\hat{S}_z + \alpha(t)\hat{S}_+ + \alpha^*(t)\hat{S}_-\right) \qquad (3.7a)$$

$$\hat{\mathrm{H}}^I{}_B = \hbar\left(\Omega_{ab}\hat{S}_0 - \omega_{ab}\hat{S}_z + \alpha^*(t)\hat{S}_+ + \alpha(t)\hat{S}_-\right) \qquad (3.7b)$$

where

$$\Omega_{ab} = \omega_a + \omega_b \qquad \omega_{ab} = \omega_a - \omega_b \qquad (3.8)$$

For a semi-classical OPO, the incident pump photon is driven by a classical external field represented by a time-dependent coupling parameter $\alpha(t)$. The external classical pump field varies harmonically with time in the form of a rotating field according to

$$\frac{d\alpha(t)}{dt} = i\omega_p \alpha \qquad (3.9)$$

which is evaluated to obtain

$$\alpha(t) = \alpha e^{-i\omega_p t} \quad ; \quad \alpha^*(t) = \alpha e^{i\omega_p t} \quad ; \quad \alpha = |\alpha(t)| = constant \qquad (3.10)$$

We substitute (3.10) in eq. (3.7a) and (3.7b) to obtain

$$\hat{H}^I{}_A(t) = \hbar\left(\Omega_{ab}\hat{S}_0 + \omega_{ab}\hat{S}_z + \alpha\{e^{-i\omega_p t}\hat{S}_+ + e^{i\omega_p t}\hat{S}_-\}\right) \qquad (3.11a)$$

$$\hat{H}^I{}_B(t) = \hbar\left(\Omega_{ab}\hat{S}_0 - \omega_{ab}\hat{S}_z + \alpha\{e^{i\omega_p t}\hat{S}_+ + e^{-i\omega_p t}\hat{S}_-\}\right) \qquad (3.11b)$$

We transform the Hamiltonian (3.11a) and (3.11b) to the rotating frame through application of unitary transformation operators defined by (Akeyo, 2008)

$$T_A(t) = e^{i\omega_p t\hat{S}_z} \quad ; \quad T_A{}^{\dagger}(t) = T_A{}^{-1}(t) = e^{-i\omega_p t S_z} \qquad (3.12a)$$

$$T_B(t) = e^{-i\omega_p t\hat{S}_z} \quad ; \quad T_B{}^{\dagger}(t) = T_B{}^{-1}(t) = e^{i\omega_p t S_z} \qquad (3.12b)$$

We evaluate (3.12a) and (3.12b) to obtain

$$T_A(t) = e^{\frac{i}{2}\omega_p t\sigma_z} = \begin{pmatrix} e^{\frac{i}{2}\omega_p t} & 0 \\ 0 & e^{-\frac{i}{2}\omega_p t} \end{pmatrix} \quad ; \quad T_A{}^{\dagger}T_A = T_A T_A{}^{\dagger} = 1 \qquad (3.13a)$$

$$T_B(t) = e^{-\frac{i}{2}\omega_p t\sigma_z} = \begin{pmatrix} e^{-\frac{i}{2}\omega_p t} & 0 \\ 0 & e^{\frac{i}{2}\omega_p t} \end{pmatrix} \quad ; \quad T_B{}^{\dagger}T_B = T_B T_B{}^{\dagger} = 1 \qquad (3.13b)$$

We express (3.5a) and (3.5b) in the rotating form as

$$i\hbar\frac{d\overline{A}}{dt} = \overline{\mathrm{H}}_A\overline{A} \qquad (3.14a)$$

$$i\hbar\frac{d\overline{B}}{dt} = \overline{\mathrm{H}}_B\overline{B} \qquad (3.14b)$$

So that under unitary transformations (equivalent to a rotation through $\omega_p t$ about the z-axis) we have (Akeyo, 2008)

$$\overline{A} = T_A\hat{A} \quad ; \quad \hat{A} = T_A{}^{\dagger}\overline{A} \quad ; \quad \overline{\mathrm{H}}_A = T_A\,\hat{H}_A{}^{I}(t)T_A{}^{\dagger} - i\hbar T_A\frac{dT_A{}^{\dagger}}{dt} \qquad (3.15a)$$

$$\overline{B} = T_B\hat{B} \quad ; \quad \hat{B} = T_B{}^{\dagger}\overline{B} \quad ; \quad \overline{\mathrm{H}}_B = T_B\,\hat{H}_B{}^{I}(t)T_B{}^{\dagger} - i\hbar T_B\frac{dT_B{}^{\dagger}}{dt} \qquad (3.15b)$$

We use (3.13a) and (3.15a) to transform the time evolution generator in (3.11a) to a rotating frame in the form

$$\overline{\mathrm{H}}_A = e^{\frac{i}{2}\omega_p t\sigma_z}\hbar\left(\Omega_{ab}\hat{S}_o + \omega_{ab}\hat{S}_z + \alpha e^{-i\omega_p t}\hat{S}_+ + \alpha e^{i\omega_p t}\hat{S}_-\right)e^{-\frac{i}{2}\omega_p t\sigma_z} - \frac{\hbar}{2}\omega_p\sigma_z \quad (3.16)$$

We express (3.16) in the form

$$\overline{\mathrm{H}}_A = \hbar\left(\Omega_{ab}T\hat{S}_o T^+ + \omega_{ab}T\hat{S}_z T^+ + \alpha e^{-i\omega_p t}T\hat{S}_+ T^+ + \alpha e^{i\omega_p t}T\hat{S}_- T^+ - \frac{1}{2}\omega_p\sigma_z\right) \quad (3.16)$$

Since $\hat{S}_0$ commutes with $\hat{S}_z$, we write

$$T\hat{S}_0 T^\dagger = \hat{S}_0 TT^\dagger = \hat{S}_0 \qquad ; \qquad T\hat{S}_z T^\dagger = \hat{S}_z TT^\dagger = \hat{S}_z \qquad (3.17a)$$

and evaluate

$$T\hat{S}_+ T^\dagger = \begin{pmatrix} e^{\frac{i}{2}\omega_p t} & 0 \\ 0 & e^{\frac{-i}{2}\omega_p t}\end{pmatrix}\begin{pmatrix}0 & 1\\ 0 & 0\end{pmatrix}\begin{pmatrix} e^{\frac{-i}{2}\omega_p t} & 0 \\ 0 & e^{\frac{i}{2}\omega_p t}\end{pmatrix} = e^{i\omega_p t}\hat{S}_+ \qquad (3.17b)$$

$$T\hat{S}_- T^\dagger = \begin{pmatrix} e^{\frac{i}{2}\omega_p t} & 0 \\ 0 & e^{\frac{-i}{2}\omega_p t}\end{pmatrix}\begin{pmatrix}0 & 0\\ 1 & 0\end{pmatrix}\begin{pmatrix} e^{\frac{-i}{2}\omega_p t} & 0 \\ 0 & e^{\frac{i}{2}\omega_p t}\end{pmatrix} = e^{-i\omega_p t}\hat{S}_+ \qquad (3.17c)$$

Eq. (3.16) is simplified by use of (3.17a-c) to obtain

$$\overline{\mathrm{H}}_A = \hbar\left(\Omega_{ab}\hat{S}_0 + \Delta\hat{S}_z + 2\alpha\hat{S}_x\right) \qquad (3.18)$$

where Ω_{ab} and $\hat{S}_x$ were defined in (3.8) and (3.6d) respectively, Δ is a constant detuning parameter defined as

$$\Delta = \omega_{ab} - \omega_p \tag{3.19}$$

Similarly, the time evolution generator in (3.11b) is transformed to the rotating frame and simplified using eq. (3.13b) and (3.15b) to obtain

$$\overline{\mathrm{H}}_B = \hbar\left(\Omega_{ab}\hat{S}_0 - \Delta\hat{S}_z + 2\alpha\hat{S}_x\right) \tag{3.20}$$

The rotating frame Hamiltonian $\overline{\mathrm{H}}_A$ and $\overline{\mathrm{H}}_B$ in (3.18) and (3.20) are time independent because the parameters Ω_{ab}, Δ and α are constant. We substitute (3.18) and (3.20) in (3.14a) and (3.14b) respectively and integrate to obtain

$$\overline{A}(t) = e^{-i\Omega_{ab}\hat{S}_0 t}\, e^{-it\left(\Delta\hat{S}_z + 2\alpha\hat{S}_x\right)}\overline{A}(0) \tag{3.21a}$$

$$\overline{B}(t) = e^{-i\Omega_{ab}\hat{S}_0 t}\, e^{-it\left(-\Delta\hat{S}_z + 2\alpha\hat{S}_x\right)}\overline{B}(0) \tag{3.21b}$$

where $\overline{A}(t)$ is time evolving photon polarization operator vector in the rotating frame for signal photon initially in horizontal polarization state and idler photon initially in vertical polarization state. $\overline{B}(t)$ is time evolving photon polarization operator vector in the rotating frame for signal photon initially in vertical polarization state and idler photon initially in horizontal polarization state.

We multiply (3.21a) by $T_A^{\dagger}(t)$ in (3.13a) from the left and use (3.15a) to transform the time evolving photon polarization operator vector back to original frame

$$\hat{A}(t) = e^{-i\Omega_{ab}\hat{S}_0 t}\, e^{-i\omega_p t\hat{S}_z}\, e^{-it\left(\Delta\hat{S}_z + \alpha(t)e^{i\omega_p t}\hat{S}_+ + \alpha^*(t)e^{-i\omega_p t}\hat{S}_-\right)}\hat{A}(0) \qquad (3.22a)$$

Similarly, we use (3.13b) and (3.15b) in (3.21b) to obtain

$$\hat{B}(t) = e^{-i\Omega_{ab}\hat{S}_0 t}\, e^{i\omega_p t\hat{S}_z}\, e^{-it\left(-\Delta\hat{S}_z + \alpha(t)e^{i\omega_p t}\hat{S}_+ + \alpha^*(t)e^{-i\omega_p t}\hat{S}_-\right)}\hat{B}(0) \qquad (3.22b)$$

The time evolution operator, U_A , is obtained from (3.22a) by writing the general form of time evolving photon polarization operator as

$$\hat{A}(t) = U_A(t)\hat{A}(0) \quad ; \qquad \hat{A}(t) = \begin{pmatrix} \hat{a}(t) \\ \hat{b}(t) \end{pmatrix} \quad , \qquad \hat{A}(0) = \begin{pmatrix} \hat{a} \\ \hat{b} \end{pmatrix} \qquad (3.23)$$

Similarly, the time evolution operator, U_B , is obtained by writing the expression

$$\hat{B}(t) = U_A(t)\hat{B}(0) \quad ; \quad \hat{B}(t) = \begin{pmatrix} \hat{b}(t) \\ \hat{a}(t) \end{pmatrix} \quad , \qquad \hat{B}(0) = \begin{pmatrix} \hat{b} \\ \hat{a} \end{pmatrix} \qquad (3.24)$$

3.2 Time evolving photon polarization state vectors

The time evolution operators, U_A and U_B, are used to construct the general time evolving photon polarization state vectors in the form

$$\left|H;t\right\rangle_a = U_A(t)\left|H\right\rangle \qquad (3.25a)$$

$$\left|V;t\right\rangle_b = U_A(t)\left|V\right\rangle \qquad (3.25b)$$

$$\left|H;t\right\rangle_b = U_B(t)\left|H\right\rangle \tag{3.25c}$$

$$\left|V;t\right\rangle_a = U_B(t)\left|V\right\rangle \tag{3.25d}$$

$\left|H;t\right\rangle_a$ and $\left|V;t\right\rangle_b$ are time evolving horizontal and vertical polarization state vectors for polarization in $\hat{A}$ and $\left|H;t\right\rangle_b$ and $\left|V;t\right\rangle_a$ are time evolving horizontal and vertical polarization state vectors arising from polarization $\hat{B}$.

3.3 Photon Polarization Bell state vectors

We use the general time evolving photon polarization state vectors (3.25a), (3.25b), (3.25c) and (3.25d) to construct photon polarization Bell state vectors in a form similar to Bell state vectors developed in (1.3a-d) for SPDC (Ling, 2008) in the general form

$$\left|\psi_+\right\rangle = \left|H;t\right\rangle_a\left|H;t\right\rangle_b + \left|V;t\right\rangle_a\left|V;t\right\rangle_b \tag{3.26a}$$

$$\left|\psi_-\right\rangle = \left|H;t\right\rangle_a\left|H;t\right\rangle_b - \left|V;t\right\rangle_a\left|V;t\right\rangle_b \tag{3.26b}$$

$$\left|\phi_+\right\rangle = \left|H;t\right\rangle_a\left|V;t\right\rangle_b + \left|V;t\right\rangle_a\left|H;t\right\rangle_b \tag{3.26c}$$

$$\left|\phi_-\right\rangle = \left|H;t\right\rangle_a\left|V;t\right\rangle_b - \left|V;t\right\rangle_a\left|H;t\right\rangle_b \tag{3.26d}$$

The time evolving photon polarization state vectors (3.25a-d) are 2x1 matrices hence the tensor products in (3.26a-d) will produce 4x1 matrices. Generally, a 4x1 matrix is represented as

$$\psi(t) = \begin{pmatrix} e \\ f \\ g \\ h \end{pmatrix} \tag{3.27}$$

where e, f, g and h are the general elements of the matrix.

3.4 Reduced density matrices and test of Bell inequality

We use reduced density matrices as an entanglement criterion and we test a Bell inequality to determine the degree of entanglement. The density matrices of photon polarization bell state vectors in (3.26a-d) are obtained using the relation (Preskil, 1998)

$$\hat{\rho}(t) = |\psi(t)\rangle\langle\psi(t)| \tag{3.28}$$

We obtain the general density matrix of photon polarization bell state vectors by using (3.27) in (3.28) to obtain a 4x4 matrix

$$\psi(t) = \begin{pmatrix} e^2 & ef & eg & eh \\ fe & f^2 & fg & fh \\ ge & gf & g^2 & gh \\ he & hf & hg & h^2 \end{pmatrix} \tag{3.29}$$

The reduced density matrix for a bipartite state for a subsystem ‘a’ is given by

$$\rho^a = tr_b(\rho^{ab}) \tag{3.30}$$

where ρ^{ab} is the density matrix of the bipartite system consisting of subsystems ‘a’ and ‘b’ whereas $tr_b(\rho^{ab})$ represents the partial trace over subsystem ‘b’. The state of a quantum system is entangled if the reduced density matrix represents a mixed state and is separable if the reduced

density matrix remains a pure state. The reduced density matrix for Bell state vectors is obtained by getting the traces of density matrices by finding the sum of the principal diagonal elements of a density matrix (Preskil, 1998). For density matrix (3.29), the trace (reduced density matrix) is

$$Tr\hat{\rho}(t) = e^2 + f^2 + g^2 + h^2 \qquad (3.31)$$

The traces of density matrices are obtained under different conditions of interaction for the pump field i.e. resonance (very strong interaction), very weak interaction, weak interaction, medium strength interaction and critical (threshold).

We use the Clauser–Horne–Shimony-Holt (CHSH) Bell inequality to test the nature of entanglement of entangled photon polarization states. We use Bell inequalities because experiments that test Bell inequality are applied to entangled photons and not with spin-1/2 objects and are easy to use. This is because the quantum state of the pair of entangled photons is not the singlet state, and the correspondence between angles and outcomes is different from that in the spin-half set-up.

The CHSH Bell inequality (Munro, Nemote and White, 2001)

$$-2 \le S \le +2 \qquad (3.32)$$

is obeyed for classical correlations. Entanglement is exhibited by violations of the Bell inequality i.e.

$$|S| > 2 \qquad (3.33)$$

The larger the violation of the Bell inequality the more the entanglement present in the system. The largest violation of the CHSH Bell inequality allowed by quantum theory was investigated by Cirel'son's and stated as Cirel'son's inequality in the form (Munro, Nemote and White, 2001)

$$\|C\| \le 2\sqrt{2} \qquad (3.34)$$

We therefore describe entanglement results of a semi-classical OPO through test of CHSH Bell inequality by use of reduced density matrices under all conditions of interaction for the pump field. Reduced density matrices are obtained from traces of density matrices using (3.31). The violation of CHSH Bell inequality (3.32) will be treated as an entangled state violation. Entanglement of polarization states arising from the semi-classical OPO will be quantified by determination of the degree of violation of CHSH Bell inequality. The greater the trace of density matrix above the trace of $|2|$ the greater the degree of entanglement of polarization states arising from the OPO. The polarization states that do not violate the Bell inequality (3.32) will be considered as weakly entangled states because Bell states are the most entangled states.

CHAPTER FOUR: RESULTS AND DISCUSSIONS

4.1 Exact solutions of Heisenberg's equations

The more general non-resonant two-mode parametric down-conversion process was studied in detail (Rekdal and Skagerstam, 1999) where the Lie algebraic method was applied to solve the equation for the time evolution operator using Schrodinger equations to obtain desired solutions in terms of fairly complicated expressions (2.16a). A simpler approach was developed (Akeyo, 2008) by considering that the basic operators of the coupled system are the annihilation and creation operators whose time evolution can be determined directly through Heisenberg's equation. In the present work, exact solutions of Heisenberg's equations arising from semi-classical OPO were obtained through substitution of Hamiltonian (1.5) directly into Heisenberg's equations (3.0). The matrix method and spin operators were used to represent time evolution generators of the system. The general time evolving polarization operator vectors were developed in (3.22a) and (3.22b) from which we identify the time evolution operators

$$U_A(t) = e^{-i\Omega_{ab}\hat{S}_0 t}\, e^{-i\omega_p t\hat{S}_z}\, e^{-it\left(\Delta\hat{S}_z+\alpha(t)e^{i\omega_p t}\hat{S}_+ +\alpha^*(t)e^{-i\omega_p t}\hat{S}_-\right)} \qquad (4.0a)$$

$$U_B(t) = e^{-i\Omega_{ab}\hat{S}_0 t}\, e^{i\omega_p t\hat{S}_z}\, e^{-it\left(-\Delta\hat{S}_z+\alpha(t)e^{i\omega_p t}\hat{S}_+ +\alpha^*(t)e^{-i\omega_p t}\hat{S}_-\right)} \qquad (4.0b)$$

Equations (4.0a-b) are simplified by expressing the first and second exponential components in matrix form

$$e^{-i\Omega_{ab}\hat{S}_0 t} = e^{-\frac{i}{2}\Omega_{ab}\sigma_0} = e^{-\frac{i}{2}\Omega_{ab}t}\mathrm{I} \qquad (4.1a)$$

$$e^{-i\omega_p t\hat{S}_z} = e^{-\frac{i}{2}\omega_p t\sigma_z} = \begin{pmatrix} e^{-\frac{i}{2}\omega_p t} & 0 \\ 0 & e^{\frac{i}{2}\omega_p t} \end{pmatrix} \qquad (4.1b)$$

$$e^{i\omega_p t\hat{S}_z} = e^{\frac{i}{2}\omega_p t\sigma_z} = \begin{pmatrix} e^{\frac{i}{2}\omega_p t} & 0 \\ 0 & e^{-\frac{i}{2}\omega_p t} \end{pmatrix} \qquad (4.1c)$$

The last exponential component in (4.0a) is evaluated by using Euler's relation

$$e^{-it\left(\Delta\hat{S}_z+\alpha(t)e^{i\omega_p t}\hat{S}_+ +\alpha^*(t)e^{-i\omega_p t}\hat{S}_-\right)} =$$

$$\cos(\beta t)\mathrm{I} - \frac{i}{\beta}\sin(\beta t)\left(\Delta\hat{S}_z+\alpha(t)e^{i\omega_p t}\hat{S}_+ +\alpha^*(t)e^{-i\omega_p t}\hat{S}_-\right) \qquad (4.2)$$

We substitute spin operators $\hat{S}_+, \hat{S}_-$ and $\hat{S}_z$ from (3.6a-b) in (4.2) to obtain

$$e^{-it\left(\Delta\hat{S}_z+\alpha(t)e^{i\omega_p t}\hat{S}_+ +\alpha^*(t)e^{-i\omega_p t}\hat{S}_-\right)} =$$

$$\begin{pmatrix} \cos(\beta t)-\frac{i\Delta}{2\beta}\sin(\beta t) & -\frac{i\alpha(t)e^{i\omega_p t}}{\beta}\sin(\beta t) \\ -\frac{i\alpha^*(t)e^{-i\omega_p t}}{\beta}\sin(\beta t) & \cos(\beta t)+\frac{i\Delta}{2\beta}\sin(\beta t) \end{pmatrix} \qquad (4.3)$$

We simplify (4.3) by writing in terms of interaction variables $\mu(t)$ and $\nu(t)$

$$e^{-it\left(\Delta\hat{S}_z+\alpha(t)e^{i\omega_p t}\hat{S}_+ +\alpha^*(t)e^{-i\omega_p t}\hat{S}_-\right)}=\begin{pmatrix} \mu(t) & \nu(t) \\ -\nu^*(t) & \mu^*(t) \end{pmatrix} \qquad (4.4)$$

where

$$\mu(t)=\cos(\beta t)-\frac{i\Delta}{2\beta}\sin(\beta t) \qquad (4.5a)$$

$$\nu(t)=-\frac{i\alpha(t)e^{i\omega_p t}}{\beta}\sin(\beta t) \qquad (4.5b)$$

$$\beta=\Delta\hat{S}_z+\alpha(t)e^{i\omega_p t}\hat{S}_+ +\alpha^*(t)e^{-i\omega_p t}\hat{S}_- \qquad (4.5c)$$

The expression in (4.5c) is evaluated by writing

$$\beta=\sqrt{\left(\Delta\hat{S}_Z+\alpha(t)e^{i\omega_p t}\hat{S}_+ +\alpha^*(t)e^{-i\omega_p t}\hat{S}_-\right)^2} \qquad (4.5d)$$

Introducing the spin operators

$$\hat{S}_+^{\,2}=0 \quad , \quad \hat{S}_-^{\,2}=0 \quad , \quad \hat{S}_Z^{\,2}=\frac{1}{4}\mathrm{I} \qquad (4.6a)$$

$$\hat{S}_Z\hat{S}_+ + \hat{S}_+\hat{S}_Z = 0 \quad , \quad \hat{S}_Z\hat{S}_- + \hat{S}_-\hat{S}_Z = 0 \quad , \quad \hat{S}_+\hat{S}_- + \hat{S}_-\hat{S}_+ = 1 \qquad (4.6b)$$

We obtain the reduced form of (4.5d)

$$\beta = \sqrt{|\alpha|^2 + \frac{\Delta^2}{4}} \qquad (4.7a)$$

This can be rewritten as

$$\beta = |\alpha|\sqrt{1+k^2} \qquad (4.7b)$$

where

$$k = \frac{\Delta}{2|\alpha|} \qquad (4.7c)$$

We substitute (4.1a), (4.1b) and (4.4) in (4.0a) to obtain exact solution of time evolution operator $U_A(t)$ in explicit form

$$U_A(t) = \begin{pmatrix} \mu(t)e^{-\frac{i}{2}(\Omega_{ab}+\omega_p)t} & \nu(t)e^{-\frac{i}{2}(\Omega_{ab}+\omega_p)t} \\ -\nu^*(t)e^{-\frac{i}{2}(\Omega_{ab}-\omega_p)t} & \mu^*(t)e^{-\frac{i}{2}(\Omega_{ab}-\omega_p)t} \end{pmatrix} \qquad (4.8)$$

Similarly, using Euler's relation and spin operators, we express the last exponential component in (4.0b) as

$$e^{-it\left(-\Delta\hat{S}_z + \alpha(t)e^{i\omega_p t}\hat{S}_+ + \alpha^*(t)e^{-i\omega_p t}\hat{S}_-\right)} = \begin{pmatrix} \mu^*(t) & -\nu^*(t) \\ \nu(t) & \mu(t) \end{pmatrix} \qquad (4.9)$$

We substitute (4.1a), (4.1c) and (4.9) in (4.0b) to obtain exact solution of time evolution operator $U_B(t)$ in explicit form

$$U_B(t)=\begin{pmatrix} \mu^*(t)e^{-\frac{i}{2}(\Omega_{ab}-\omega_p)t} & -\nu^*(t)e^{-\frac{i}{2}(\Omega_{ab}-\omega_p)t} \\ \nu(t)e^{-\frac{i}{2}(\Omega_{ab}+\omega_p)t} & \mu(t)e^{-\frac{i}{2}(\Omega_{ab}+\omega_p)t} \end{pmatrix} \qquad (4.10)$$

The expressions (4.8) and (4.10) are the required exact solutions in explicit form of time evolution operators for the dynamics of the semi-classical OPO obtained within the Heisenberg picture and which we use to obtain the general time evolving polarization state vectors.

We substitute the exact solution of time evolution operator (4.8) into (3.25a) and (3.25b) and evaluate to obtain

$$\left|H;t\right\rangle_a = \left(\mu(t)e^{-\frac{i}{2}\left(\Omega_{ab}+\omega_p\right)t}\left|0\right\rangle - \nu^*(t)e^{-\frac{i}{2}\left(\Omega_{ab}-\omega_p\right)t}\left|1\right\rangle \right) \quad , \quad (4.11a)$$

$$\left|V;t\right\rangle_b = \left(\nu(t)e^{-\frac{i}{2}\left(\Omega_{ab}+\omega_p\right)t}\left|0\right\rangle + \mu^*(t)e^{-\frac{i}{2}\left(\Omega_{ab}-\omega_p\right)t}\left|1\right\rangle \right) \quad (4.11b)$$

Similarly, we substitute the exact solution of time evolution operator (4.10) into (3.25c) and (3.25d) and evaluate to obtain

$$\left|H;t\right\rangle_b = \left(\mu^*(t) e^{-\frac{i}{2}\left(\Omega_{ab}-\omega_p\right)t} \left|0\right\rangle + \nu(t) e^{-\frac{i}{2}\left(\Omega_{ab}+\omega_p\right)t} \left|1\right\rangle \right) \quad (4.11c)$$

$$\left|V;t\right\rangle_a = \left(-\nu^*(t) e^{-\frac{i}{2}\left(\Omega_{ab}-\omega_p\right)t} \left|0\right\rangle + \mu(t) e^{-\frac{i}{2}\left(\Omega_{ab}+\omega_p\right)t} \left|1\right\rangle \right) \quad (4.11d)$$

Equations (4.11a) and (4.11d) are exact and explicit solutions of general time evolving horizontal and vertical polarization state vectors for the signal photon while (4.11c) and (4.11b) are exact and explicit solutions of general time evolving horizontal and vertical photon polarization state vectors for the idler photon. The solutions are used to determine photon polarization Bell state vectors.

4.2 Photon polarization Bell state vectors

We use the general time evolving polarization state vectors of signal and idler photons in the semi-classical OPO obtained in (4.11a) and (4.11c) together with the inner products

$$\left|0\right\rangle\left\langle 0\right| = \begin{pmatrix} 1 \\ 0 \\ 0 \\ 0 \end{pmatrix} \quad , \quad \left|0\right\rangle\left\langle 1\right| = \begin{pmatrix} 0 \\ 1 \\ 0 \\ 0 \end{pmatrix} \quad , \qquad (4.12a)$$

$$|1\rangle\langle 0| = \begin{pmatrix} 0 \\ 0 \\ 1 \\ 0 \end{pmatrix} \quad , \quad |1\rangle\langle 1| = \begin{pmatrix} 0 \\ 0 \\ 0 \\ 1 \end{pmatrix} \quad , \qquad (4.12b)$$

to evaluate the tensor product

$$|H;t\rangle_a |H;t\rangle_b =$$

$$e^{-i\Omega_{ab}t}\left(|\mu(t)|^2 \begin{pmatrix} 1 \\ 0 \\ 0 \\ 0 \end{pmatrix} + \mu(t)\nu(t)e^{-i\omega_p t}\begin{pmatrix} 0 \\ 1 \\ 0 \\ 0 \end{pmatrix} - \nu^*(t)\mu^*(t)e^{i\omega_p t}\begin{pmatrix} 0 \\ 0 \\ 1 \\ 0 \end{pmatrix} - |\nu(t)|^2 \begin{pmatrix} 0 \\ 0 \\ 0 \\ 1 \end{pmatrix} \right) \quad (4.12c)$$

Eq. (4.12c) reduces to

$$|H;t\rangle_a |H;t\rangle_b = e^{-i\Omega_{ab}t}\begin{pmatrix} |\mu(t)|^2 \\ \mu(t)\nu(t)e^{-i\omega_p t} \\ -\nu^*(t)\mu^*(t)e^{i\omega_p t} \\ -|\nu(t)|^2 \end{pmatrix} \qquad (4.13a)$$

Similarly, we use the general time evolving polarization state vectors of signal and idler photons in (4.11b) and (4.11d) to obtain

$$|V;t\rangle_a|V;t\rangle_b = e^{-i\Omega_{ab}t}\begin{pmatrix} -|\nu(t)|^2 \\ -\nu^*(t)\mu^*(t)e^{i\omega_p t} \\ \mu(t)\nu(t)e^{-i\omega_p t} \\ |\mu(t)|^2 \end{pmatrix} \quad , \qquad (4.13b)$$

We use the general time evolving polarization state vectors of signal and idler photons in (4.11a) and (4.11b) to obtain

$$|H;t\rangle_a|V;t\rangle_b = e^{-i\Omega_{ab}t}\begin{pmatrix} \mu(t)\nu(t)e^{-i\omega_p t} \\ |\mu(t)|^2 \\ -|\nu(t)|^2 \\ -\nu^*(t)\mu^*(t)e^{i\omega_p t} \end{pmatrix} \quad , \qquad (4.13c)$$

and finally we use the general time evolving polarization state vectors of signal and idler photons in (4.11c) and (4.11d) to obtain

$$|V;t\rangle_a|H;t\rangle_b = e^{-i\Omega_{ab}t}\begin{pmatrix} -\nu^*(t)\mu^*(t)e^{i\omega_p t} \\ -|\nu(t)|^2 \\ |\mu(t)|^2 \\ \mu(t)\nu(t)e^{-i\omega_p t} \end{pmatrix} \qquad (4.13d)$$

We substitute equations (4.13a) and (4.13b) in equations (3.26a) to obtain the time evolving Bell state vector in the form

$$\left|\psi_{+}\right\rangle = e^{-i\Omega_{ab}t}\begin{pmatrix} |\mu(t)|^2 - |\nu(t)|^2 \\ \mu(t)\nu(t)e^{-i\omega_p t} - \nu^*(t)\mu^*(t)e^{i\omega_p t} \\ -\nu^*(t)\mu^*(t)e^{i\omega_p t} + \mu(t)\nu(t)e^{-i\omega_p t} \\ -|\nu(t)|^2 + |\mu(t)|^2 \end{pmatrix} \qquad (4.14a)$$

Similarly, we use equations (4.13a) and (4.13b) in equations (3.26b) to obtain the time evolving Bell state vector in the form

$$\left|\psi_{-}\right\rangle = e^{-i\Omega_{ab}t}\begin{pmatrix} |\mu(t)|^2 + |\nu(t)|^2 \\ \mu(t)\nu(t)e^{-i\omega_p t} + \nu^*(t)\mu^*(t)e^{i\omega_p t} \\ -\nu^*(t)\mu^*(t)e^{i\omega_p t} - \mu(t)\nu(t)e^{-i\omega_p t} \\ -|\nu(t)|^2 - |\mu(t)|^2 \end{pmatrix} \quad , \qquad (4.14b)$$

we substitute equations (4.13c) and (4.13d) in equations (3.26c) to obtain the time evolving Bell state vector in the form

$$\left|\phi_{+}\right\rangle = e^{-i\Omega_{ab}t}\begin{pmatrix} \mu(t)\nu(t)e^{-i\omega_p t} - \nu^*(t)\mu^*(t)e^{i\omega_p t} \\ |\mu(t)|^2 - |\nu(t)|^2 \\ -|\nu(t)|^2 + |\mu(t)|^2 \\ -\nu^*(t)\mu^*(t)e^{i\omega_p t} + \mu(t)\nu(t)e^{-i\omega_p t} \end{pmatrix} \quad , \qquad (4.14c)$$

and finally we use equations (4.13c) and (4.13d) in equations (3.26d) to obtain the time evolving Bell state vector in the form

$$\left|\phi_{-}\right\rangle = e^{-i\Omega_{ab}t}\begin{pmatrix} \mu(t)\nu(t)e^{-i\omega_p t} + \nu^*(t)\mu^*(t)e^{i\omega_p t} \\ |\mu(t)|^2 + |\nu(t)|^2 \\ -|\nu(t)|^2 - |\mu(t)|^2 \\ -\nu^*(t)\mu^*(t)e^{i\omega_p t} - \mu(t)\nu(t)e^{-i\omega_p t} \end{pmatrix} \qquad (4.14d)$$

We substitute interaction variables (4.5a) and (4.5b) into (4.14a), (4.14b), (4.14c) and (4.14d) and using (3.10) we obtain

$$\left|\psi_{+}\right\rangle = e^{-i\Omega_{ab}t}\begin{pmatrix} \cos^2(\beta t) - \left(\frac{\Delta^2 + 4|\alpha(t)|^2}{4\beta^2}\right)\sin^2(\beta t) \\ \frac{-i(\alpha(t)+\alpha^*(t))}{2\beta}\sin(2\beta t) + \frac{\Delta(\alpha^*(t)-\alpha(t))}{2\beta^2}\sin^2(\beta t) \\ \frac{-i(\alpha(t)+\alpha^*(t))}{2\beta}\sin(2\beta t) + \frac{\Delta(\alpha^*(t)-\alpha(t))}{2\beta^2}\sin^2(\beta t) \\ \cos^2(\beta t) - \left(\frac{\Delta^2 + 4|\alpha(t)|^2}{4\beta^2}\right)\sin^2(\beta t) \end{pmatrix}, \qquad (4.15a)$$

$$\left|\psi_{-}\right\rangle = e^{-i\Omega_{ab}t}\begin{pmatrix} \cos^2(\beta t) - \left(\frac{\Delta^2 - 4|\alpha(t)|^2}{4\beta^2}\right)\sin^2(\beta t) \\ \frac{i(\alpha^*(t)-\alpha(t))}{2\beta}\sin(2\beta t) - \frac{\Delta(\alpha(t)+\alpha^*(t))}{2\beta^2}\sin^2(\beta t) \\ -\frac{i(\alpha^*(t)-\alpha(t))}{2\beta}\sin(2\beta t) + \frac{\Delta(\alpha(t)+\alpha^*(t))}{2\beta^2}\sin^2(\beta t) \\ -\cos^2(\beta t) + \left(\frac{\Delta^2 - 4|\alpha(t)|^2}{4\beta^2}\right)\sin^2(k\beta t) \end{pmatrix}, \quad (4.15b)$$

$$\left|\phi_{+}\right\rangle = e^{-i\Omega_{ab}t}\begin{pmatrix} \frac{-i(\alpha(t)+\alpha^*(t))}{2\beta}\sin(2\beta t) + \frac{\Delta(\alpha^*(t)-\alpha(t))}{2\beta^2}\sin^2(\beta t) \\ \cos^2(\beta t) - \left(\frac{\Delta^2 + 4|\alpha(t)|^2}{4\beta^2}\right)\sin^2(\beta t) \\ \cos^2(\beta t) - \left(\frac{\Delta^2 + 4|\alpha(t)|^2}{4\beta^2}\right)\sin^2(\beta t) \\ \frac{-i(\alpha(t)+\alpha^*(t))}{2\beta}\sin(2\beta t) + \frac{\Delta(\alpha^*(t)-\alpha(t))}{2\beta^2}\sin^2(\beta t) \end{pmatrix}, \quad (4.15c)$$

and

$$\left|\phi_{-}\right\rangle = e^{-i\Omega_{ab}t}\begin{pmatrix} \frac{i(\alpha^{*}(t)-\alpha(t))}{2\beta}\sin(2\beta t) - \frac{\Delta(\alpha(t)+\alpha^{*}(t))}{2\beta^{2}}\sin^{2}(\beta t) \\ \cos^{2}(\beta t) - \left(\frac{\Delta^{2}-4\left|\alpha(t)\right|^{2}}{4\beta^{2}}\right)\sin^{2}(\beta t) \\ -\cos^{2}(\beta t) + \left(\frac{\Delta^{2}-4\left|\alpha(t)\right|^{2}}{4\beta^{2}}\right)\sin^{2}(\beta t) \\ \frac{-i(\alpha^{*}(t)-\alpha(t))}{2\beta}\sin(2\beta t) + \frac{\Delta(\alpha(t)+\alpha^{*}(t))}{2\beta^{2}}\sin^{2}(\beta t) \end{pmatrix} \qquad (4.15d)$$

We use (3.10) and the following trigonometric identity relations

$$2\cos\omega_{p}t = e^{i\omega_{p}t} + e^{-i\omega_{p}t} \qquad (4.16a)$$

$$2i\sin\omega_{p}t = e^{i\omega_{p}t} - e^{-i\omega_{p}t} \qquad (4.16b)$$

in (4.15a-d) to transform the Bell states in explicit form

$$\left|\psi_{+}\right\rangle = e^{-i\Omega_{ab}t}\begin{pmatrix} \cos^{2}(\beta t) - \left(\frac{\Delta^{2}+4\left|\alpha(t)\right|^{2}}{4\beta^{2}}\right)\sin^{2}(\beta t) \\ -\frac{i\alpha}{\beta}\cos(\omega_{p}t)\sin(2\beta t) + \frac{i\Delta\alpha}{\beta^{2}}\sin(\omega_{p}t)\sin^{2}(\beta t) \\ -\frac{i\alpha}{\beta}\cos(\omega_{p}t)\sin(2\beta t) + \frac{i\Delta\alpha}{\beta^{2}}\sin(\omega_{p}t)\sin^{2}(\beta t) \\ \cos^{2}(\beta t) - \left(\frac{\Delta^{2}+4\left|\alpha(t)\right|^{2}}{4\beta^{2}}\right)\sin^{2}(\beta t) \end{pmatrix}, \qquad (4.17a)$$

$$\left|\psi_{-}\right\rangle = e^{-i\Omega_{ab}t}\begin{pmatrix} \cos^2(\beta t) - \left(\frac{\Delta^2 - 4|\alpha(t)|^2}{4\beta^2}\right)\sin^2(\beta t) \\ -\frac{\alpha}{\beta}\sin(\omega_p t)\sin(2\beta t) - \frac{\Delta\alpha}{\beta^2}\cos(\omega_p t)\sin^2(\beta t) \\ \frac{\alpha}{\beta}\sin(\omega_p t)\sin(2\beta t) + \frac{\Delta\alpha}{\beta^2}\cos(\omega_p t)\sin^2(\beta t) \\ -\cos^2(\beta t) + \left(\frac{\Delta^2 - 4|\alpha(t)|^2}{4\beta^2}\right)\sin^2(\beta t) \end{pmatrix}, \quad (4.17b)$$

$$\left|\phi_{+}\right\rangle = e^{-i\Omega_{ab}t}\begin{pmatrix} -\frac{i\alpha}{\beta}\cos(\omega_p t)\sin(2\beta t) + \frac{i\Delta\alpha}{\beta^2}\sin(\omega_p t)\sin^2(\beta t) \\ \cos^2(\beta t) - \left(\frac{\Delta^2 + 4|\alpha(t)|^2}{4\beta^2}\right)\sin^2(\beta t) \\ \cos^2(\beta t) - \left(\frac{\Delta^2 + 4|\alpha(t)|^2}{4\beta^2}\right)\sin^2(\beta t) \\ -\frac{i\alpha}{\beta}\cos(\omega_p t)\sin(2\beta t) + \frac{i\Delta\alpha}{\beta^2}\sin(\omega_p t)\sin^2(\beta t) \end{pmatrix}, \quad (4.17c)$$

and

$$\left|\phi_{-}\right\rangle = e^{-i\Omega_{ab}t}\begin{pmatrix} -\frac{\alpha}{\beta}\sin(\omega_p t)\sin(2\beta t) - \frac{\Delta\alpha}{\beta^2}\cos(\omega_p t)\sin^2(\beta t) \\ \cos^2(\beta t) - \left(\frac{\Delta^2 - 4|\alpha(t)|^2}{4\beta^2}\right)\sin^2(\beta t) \\ -\cos^2(\beta t) + \left(\frac{\Delta^2 - 4|\alpha(t)|^2}{4\beta^2}\right)\sin^2(\beta t) \\ \frac{\alpha}{\beta}\sin(\omega_p t)\sin(2\beta t) + \frac{\Delta\alpha}{\beta^2}\cos(\omega_p t)\sin^2(\beta t) \end{pmatrix} \quad (4.17d)$$

Equations (4.17a-d) are exact and explicit solutions of general time evolving Photon polarization Bell state vectors arising from semi-classical OPO. The solutions (4.17a-d) are detailed and evolving with time than the simple Bell states presented in (1.3a-d), (1.6) and (2.9). The time evolving Bell state vectors (4.17a-d) were used for test of entanglement in the reduced density matrices and Bell inequalities, under different conditions of interaction.

4.3 Reduced density matrices and Test of Bell inequality

4.3.1 Reduced density matrices at resonance

At resonance, the condition $|\alpha| >> \Delta$ is considered and (4.7b) reduces to

$$\beta = |\alpha| \qquad ; \qquad k = 0 \tag{4.18}$$

We use (4.18) in Bell state (4.17a) and simplify to obtain

$$|\psi_+\rangle = e^{-i\Omega_{ab}t}\begin{pmatrix} \cos(2|\alpha|t) \\ -i\cos(\omega_p t)\sin(2|\alpha|t) \\ -i\cos(\omega_p t)\sin(2|\alpha|t) \\ \cos(2|\alpha|t) \end{pmatrix} \tag{4.19a}$$

We substitute (4.19a) into (3.28) to obtain the density matrix

$$\hat{\rho}_+(t) = |\psi_+(t)\rangle\langle\psi_+(t)|$$

$$= \begin{pmatrix} \cos^2(2|\alpha|t) & \frac{i}{2}\cos(\omega_p t)\sin(4|\alpha|t) & \frac{i}{2}\cos(\omega_p t)\sin(4|\alpha|t) & \cos^2(2|\alpha|t) \\ \frac{-i}{2}\cos(\omega_p t)\sin(4|\alpha|t) & \cos^2(\omega_p t)\sin^2(2|\alpha|t) & \cos^2(\omega_p t)\sin^2(2|\alpha|t) & \frac{-i}{2}\cos(\omega_p t)\sin(4|\alpha|t) \\ \frac{-i}{2}\cos(\omega_p t)\sin(4|\alpha|t) & \cos^2(\omega_p t)\sin^2(2|\alpha|t) & \cos^2(\omega_p t)\sin^2(2|\alpha|t) & \frac{-i}{2}\cos(\omega_p t)\sin(4|\alpha|t) \\ \cos^2(2|\alpha|t) & \frac{i}{2}\cos(\omega_p t)\sin(4|\alpha|t) & \frac{i}{2}\cos(\omega_p t)\sin(4|\alpha|t) & \cos^2(2|\alpha|t) \end{pmatrix} \tag{4.19b}$$

Taking (4.19b) equal to (3.29), we use (3.31) to obtain the trace of density matrix

$$Tr\hat{\rho}_{+}(t) = 2 - 2\sin^2(\omega_p t)\sin^2(2|\alpha|t) \qquad (4.19c)$$

At

$$t = \frac{n\pi}{\omega_p} \quad , \quad \omega_p = 2|\alpha| \quad ; \qquad \text{n=0,1,2,....} \qquad (4.19d)$$

the trace in (4.19c) is greatest i.e. the trace=2.

At

$$t = \left(\frac{1}{2} + n\right)\frac{\pi}{\omega_p} \qquad ; \qquad \omega_p = 2|\alpha| \qquad \text{n=0, 1, 2...} \qquad (4.19e)$$

the trace in (4.19c) is least i.e. trace=0.

In general, the trace (4.19c) for Bell state vector (3.26a) at resonance does not violate the CHSH Bell inequality (3.32) hence a weak entanglement is produced at the time (4.19d) and a weaker entanglement at the time (4.19e).

We observe that entanglement of a Bell state vector (3.26a) under resonance for semi-classical OPO is dynamic and can be best utilized for practical implementation of quantum communication protocols at the time (4.19d).

Similarly, we use (4.18) in (4.17b) to obtain

$$\left|\psi_{-}\right\rangle = e^{-i\Omega_{ab}t}\begin{pmatrix} 1 \\ -\sin(\omega_p t)\sin(2|\alpha|t) \\ \sin(\omega_p t)\sin(2|\alpha|t) \\ -1 \end{pmatrix} \qquad (4.20a)$$

Taking (4.20a) equal to (3.27), we use (3.31) to obtain the trace of density matrix $\hat{\rho}_{-}(t) = |\psi_{-}(t)\rangle\langle\psi_{-}(t)|$ as

$$Tr\hat{\rho}_{-}(t) = 2 + 2\sin^2(\omega_p t)\sin^2(2|\alpha|t) \qquad (4.20b)$$

At

$$t = \frac{n\pi}{\omega_p} \quad , \quad \omega_p = 2|\alpha| \quad ; \quad \text{n=0,1,2,....} \qquad (4.20c)$$

the trace in (4.20b) is least i.e. trace=2.

At

$$t = \left(\frac{1}{2} + n\right)\frac{\pi}{\omega_p} \quad , \quad \omega_p = 2|\alpha| \quad ; \quad \text{n=0, 1, 2...} \qquad (4.20d)$$

the trace in (4.20c) is greatest i.e. trace=4.

The trace (4.20b) for Bell state vector (3.26b) at resonance does not violate the CHSH Bell inequality (3.32) at the time (4.20c) hence a weak entanglement is produced. The trace in (4.20b) violates the CHSH Bell inequality (3.32) at the time (4.20d) hence a stronger entanglement is achieved above the Cirel'son's inequality of $2\sqrt{2}$ (Munro, Nemote and White, 2001).

It is observed that the entanglement of Bell state vector (3.26b) under resonance for a semi-classical OPO is dynamic and can be best utilized for practical implementation of quantum communication protocols at the time in (4.20d).

We use (4.18) in (4.17c) to obtain

$$\left|\phi_{+}\right\rangle = e^{-i\Omega_{ab}t}\begin{pmatrix} -i\cos(\omega_p t)\sin(2|\alpha|t) \\ \cos(2|\alpha|t) \\ \cos(2|\alpha|t) \\ -i\cos(\omega_p t)\sin(2|\alpha|t) \end{pmatrix} \qquad (4.21a)$$

Taking (4.21a) equal to (3.27), we use (3.31) to obtain the trace of density matrix

$\hat{\rho}_{+}(t) = \left|\phi_{+}(t)\right\rangle\left\langle\phi_{+}(t)\right|$ as

$$Tr\hat{\rho}_{-}(t) = 2 - 2\sin^2(\omega_p t)\sin^2(2|\alpha|t) \qquad (4.21b)$$

The trace (4.21b) is similar to the trace (4.19c). Entanglement properties for Bell state vector (3.26c) under resonance for semi-classical OPO are similar to those of Bell state vector (3.26a) described in (4.19d-e).

We use (4.18) in (4.17d) to obtain

$$\left|\phi_{-}\right\rangle = e^{-i\Omega_{ab}t}\begin{pmatrix} -\sin(\omega_p t)\sin(2|\alpha|t) \\ 1 \\ -1 \\ \sin(\omega_p t)\sin(2|\alpha|t) \end{pmatrix} \qquad (4.22a)$$

Taking (4.22a) equal to (3.27), we use (3.31) to obtain the trace of density matrix

$\hat{\rho}_{-}(t) = \left|\phi_{-}(t)\right\rangle\left\langle\phi_{-}(t)\right|$ as

$$Tr\hat{\rho}_{-}(t) = 2 + 2\sin^2(\omega_p t)\sin^2(2|\alpha|t) \qquad (4.22b)$$

The trace (4.22b) is similar to the trace (4.20b). Entanglement properties for Bell state vector (3.26d) under resonance for semi-classical OPO are similar to those of Bell state vector (3.26b) described in (4.20c-d).

4.3.2 Reduced density matrices at very weak interaction

For a case of very weak interaction we consider the condition $\Delta >> |\alpha|$ and (4.7b) reduces to

$$\beta = |\alpha| k \quad ; \quad k >> 1 \qquad (4.23)$$

We substitute (4.23) in (4.17a) and simplify to obtain

$$\left|\psi_+\right\rangle = e^{-i\Omega_{ab}t}\begin{pmatrix} \cos(2|\alpha|kt) - \frac{1}{k^2}\sin^2(|\alpha|kt) \\ -\frac{i}{k}\cos(\omega_p t)\sin(2\beta t) + \frac{2i}{k}\sin(\omega_p t)\sin^2(\beta t) \\ -\frac{i}{k}\cos(\omega_p t)\sin(2\beta t) + \frac{2i}{k}\sin(\omega_p t)\sin^2(\beta t) \\ \cos(2|\alpha|kt) - \frac{1}{k^2}\sin^2(|\alpha|kt) \end{pmatrix} \quad , \quad (4.24a)$$

Considering at a very weak interaction, (4.24a) reduces to

$$\left|\psi_+\right\rangle = e^{-i\Omega_{ab}t}\begin{pmatrix} \cos(2|\alpha|kt) \\ 0 \\ 0 \\ \cos(2|\alpha|kt) \end{pmatrix} \quad , \qquad (4.24b)$$

Taking (4.24b) equal to (3.27), we use (3.31) to obtain the trace of density matrix

$\hat{\rho}_+(t) = \left|\psi_+(t)\right\rangle\left\langle\psi_+(t)\right|$ as

$$Tr\hat{\rho}_{+}(t) = 2 - 2\sin^2(2|\alpha|kt) \qquad (4.24c)$$

At

$$t = \frac{n\pi}{2|\alpha|k} \quad ; \quad \text{n=0,1,2,....} \quad ; \quad k >> 1 \qquad (4.24d)$$

the trace in (4.24c) is greatest i.e. trace=2.

At

$$t = \left(\frac{1}{2} + n\right)\frac{\pi}{2|\alpha|k} ; \quad \text{n=0, 1, 2...} \quad ; \quad k >> 1 \qquad (4.24e)$$

the trace in (4.24c) is least i.e. trace=0.

The trace (4.24c) for Bell state vector (3.26a) at very weak interaction does not violate the CHSH Bell inequality (3.32) hence a weak entanglement is produced at the time (4.24e) and a weaker entanglement at the time (4.24d).

We observe that entanglement of a Bell state vector (3.26a) under very weak interaction for semi-classical OPO is dynamic and can be best utilized for practical implementation of quantum communication protocols at the time (4.24d).

Similarly, we use (4.23) in (4.17b) to obtain

$$\left|\psi_{-}\right\rangle = e^{-i\Omega_{ab}t}\begin{pmatrix} \cos(2|\alpha|kt)+\frac{1}{k^2}\sin^2(|\alpha|kt) \\ -\frac{1}{k}\sin(\omega_p t)\sin(2|\alpha|kt)-\frac{2}{k}\cos(\omega_p t)\sin^2(|\alpha|kt) \\ \frac{1}{k}\sin(\omega_p t)\sin(2|\alpha|kt)+\frac{2}{k}\cos(\omega_p t)\sin^2(|\alpha|kt) \\ -\cos(2|\alpha|kt)+\frac{1}{k^2}\sin^2(|\alpha|kt) \end{pmatrix} \quad , \quad (4.25a)$$

At a very weak interaction $k >> 1$, (4.25a) reduces to

$$\left|\psi_{+}\right\rangle = e^{-i\Omega_{ab}t}\begin{pmatrix} \cos(2|\alpha|kt) \\ 0 \\ 0 \\ -\cos(2|\alpha|kt) \end{pmatrix} \quad , \quad (4.25b)$$

Taking (4.25b) equal to (3.27), we use (3.31) to obtain the trace of density matrix

$\hat{\rho}_{+}(t) = \left|\psi_{+}(t)\right\rangle\left\langle\psi_{+}(t)\right|$ as

$$Tr\hat{\rho}_{+}(t) = 2 - 2\sin^2(2|\alpha|kt) \quad (4.25c)$$

The trace (4.25c) is similar to the trace (4.24c). Entanglement properties for Bell state vector (3.26b) under very strong interaction for semi-classical OPO are similar to those of Bell state vector (3.26a) described above in (4.24d-e).

We use (4.23) in (4.17c) to obtain

$$\left|\phi_{+}\right\rangle = e^{-i\Omega_{ab}t}\begin{pmatrix} -\frac{i}{k}\cos(\omega_p t)\sin(2|\alpha|kt)+\frac{2i}{k}\sin(\omega_p t)\sin^2(|\alpha|kt) \\ \cos(2|\alpha|kt)-\frac{1}{k^2}\sin^2(|\alpha|kt) \\ \cos(2|\alpha|kt)-\frac{1}{k^2}\sin^2(|\alpha|kt) \\ \frac{-i}{k}\cos(\omega_p t)\sin 2(|\alpha|kt)+\frac{2i}{k}\sin(\omega_p t)\sin^2(|\alpha|kt) \end{pmatrix} \quad (4.26a)$$

At a very weak interaction $k >> 1$, (4.26a) reduces to

$$\left|\psi_{+}\right\rangle = e^{-i\Omega_{ab}t}\begin{pmatrix} 0 \\ \cos(2|\alpha|kt) \\ \cos(2|\alpha|kt) \\ 0 \end{pmatrix} \quad , \quad (4.26b)$$

Taking (4.26b) equal to (3.27), we use (3.31) to obtain the trace of density matrix

$\hat{\rho}_{+}(t) = \left|\phi_{+}(t)\right\rangle\left\langle\phi_{+}(t)\right|$ as

$$Tr\hat{\rho}_{+}(t) = 2 - 2\sin^2(2|\alpha|kt) \qquad (4.26c)$$

The trace (4.26c) is similar to the trace (4.24c). The entanglement properties for Bell state vector (3.26c) under very strong interaction for semi-classical OPO are similar to those of Bell state vector (3.26a) described above in (4.24d-e).

We use (4.23) in (4.17d) to obtain

$$\left|\phi_{-}\right\rangle = e^{-i\Omega_{ab}t}\begin{pmatrix} -\frac{i}{k}\sin(\omega_p t)\sin(2|\alpha|kt) - \frac{2}{k}\cos(\omega_p t)\sin^2(|\alpha|kt) \\ \cos(2|\alpha|kt) + \frac{1}{k^2}\sin^2(|\alpha|kt) \\ -\cos(2|\alpha|kt) + \frac{1}{k^2}\sin^2(|\alpha|kt) \\ \frac{i}{k}\sin(\omega_p t)\sin(2|\alpha|kt) + \frac{2}{k}\cos(\omega_p t)\sin^2(|\alpha|kt) \end{pmatrix} \quad (4.27a)$$

At a very weak interaction $k >> 1$, (4.27a) reduces to

$$\left|\psi_{+}\right\rangle = e^{-i\Omega_{ab}t}\begin{pmatrix} 0 \\ \cos(2|\alpha|kt) \\ -\cos(2|\alpha|kt) \\ 0 \end{pmatrix} \quad , \quad (4.27b)$$

Taking (4.27b) equal to (3.27), we use (3.31) to obtain the trace of density matrix

$\hat{\rho}_{-}(t) = \left|\phi_{-}(t)\right\rangle\left\langle\phi_{-}(t)\right|$ as

$$Tr\hat{\rho}_{+}(t) = 2 - 2\sin^2(2|\alpha|kt) \qquad (4.27c)$$

The trace (4.27c) is similar to the trace (4.24c). The entanglement properties for Bell state vector (3.26d) under very weak interaction for semi-classical OPO are similar to those of Bell state vector (3.26b) described above in (4.24d-e).

4.3.3 Reduced density matrices at weak interaction, medium strength and critical (threshold) interaction

The cases of weak interaction, medium strength interaction and critical (threshold) interaction are satisfied under the conditions $\Delta > |\alpha|, \Delta < |\alpha|$ and $\Delta = |\alpha|$ respectively and (4.7b) is represented as

$$\beta = |\alpha|\sqrt{1+k^2} \qquad ; \qquad k>1 \quad , \qquad k<1 \quad , \qquad k=1/2 \tag{4.28}$$

We substitute (4.28) in (4.17a) and simplify to obtain

$$\left|\psi_+\right\rangle = e^{-i\Omega_{ab}t}\begin{pmatrix} \cos(2|\alpha|t\sqrt{1+k^2}) \\ \frac{-i}{\sqrt{1+k^2}}\cos(\omega_p t)\sin(2|\alpha|t\sqrt{1+k^2}) + \frac{2ik}{(1+k^2)}\sin(\omega_p t)\sin^2(|\alpha|t\sqrt{1+k^2}) \\ \frac{-i}{\sqrt{1+k^2}}\cos(\omega_p t)\sin(2|\alpha|t\sqrt{1+k^2}) + \frac{2ik}{(1+k^2)}\sin(\omega_p t)\sin^2(|\alpha|t\sqrt{1+k^2}) \\ \cos(2|\alpha|t\sqrt{1+k^2}) \end{pmatrix} \tag{4.29a}$$

where

$$\frac{\Delta^2 + 4|\alpha(t)|^2}{4\beta^2} = 1 \tag{4.29c}$$

$$k>1 \quad , \qquad k<1 \quad , \qquad k=1/2 \tag{4.29b}$$

for weak interaction, medium strength interaction and critical (threshold) interaction respectively.

Taking (4.29a) equal to (3.27), we determine the density matrix $\hat{\rho}_+(t) = \left|\psi_+(t)\right\rangle\left\langle\psi_+(t)\right|$ and use (3.31) to obtain the trace

$$Tr\hat{\rho}_{+}(t) = 2 - 2\sin^2(2|\alpha|t\sqrt{1+k^2}) + \frac{2}{(1+k^2)}\cos^2(\omega_p t)\sin^2(2|\alpha|t\sqrt{1+k^2}) -$$

$$\frac{8k}{(1+k^2)^{\frac{3}{2}}}\cos(\omega_p t)\sin(2|\alpha|t\sqrt{1+k^2})\sin(\omega_p t)\sin^2(|\alpha|t\sqrt{1+k^2}) +$$

$$\frac{8k^2}{(1+k^2)^2}\sin^2(\omega_p t)\sin^4(|\alpha|t\sqrt{1+k^2}) \qquad (4.29c)$$

At

$$t = \frac{n\pi}{|\alpha|\sqrt{1+k^2}} \quad ; \qquad \text{n=0, 1, 2…} \qquad (4.29d)$$

the trace in (4.29c) is least i.e. the trace=2.

At

$$t = \left(\frac{1}{2} + n\right)\frac{\pi}{\omega_p} \quad ; \quad \omega_p = |\alpha|\sqrt{1+k^2} \quad ; \quad \text{n=0, 1, 2…} \qquad (4.29e)$$

the trace in (4.29c) is greatest i.e.

$$Tr\hat{\rho}_{+}(t) = 2 + \frac{8k^2}{(1+k^2)^2} \qquad (4.29f)$$

The trace (4.29c) for Bell state vector (3.26a) under weak interaction, medium strength and critical interaction at k>1, k<1 and k=1/2 respectively does not violate the CHSH Bell inequality (3.32) at the time (4.29d) hence produces a weak entanglement.

The trace (4.29c) violates the CHSH Bell inequality (3.32) for Bell state vector (3.26a) hence producing a strong entanglement above the Cirel'son's inequality projection of $2\sqrt{2}$ at the time (4.29e). The greatest trace at k>1 under weak interaction is less than 4, the greatest trace at k<1

under medium strength is 4 and the greatest trace at k=1/2 under critical interaction is 3.28. The trace (4.29f) at weak and medium strength interaction reduces as the value of k moves away from 1 i.e. k>1 or k<1.

It is observed that entanglement of a Bell state vector in (3.26a) for semi-classical OPO under weak interaction, medium strength and critical interaction is dynamical and can be best utilized for practical implementation of quantum communication protocols at the time in (4.29e) when entanglement is greater.

Similarly, we use (4.28) in (4.17b) to obtain

$$\left|\psi_{-}\right\rangle = e^{-i\Omega_{ab}t}\begin{pmatrix} \cos^2(|\alpha|t\sqrt{1+k^2}) - \left(\frac{k^2-1}{k^2+1}\right)\sin^2(|\alpha|t\sqrt{1+k^2}) \\ -\frac{1}{\sqrt{1+k^2}}\sin(\omega_p t)\sin(2|\alpha|t\sqrt{1+k^2}) - \frac{2k}{(1+k^2)}\cos(\omega_p t)\sin^2(|\alpha|t\sqrt{1+k^2}) \\ \frac{1}{\sqrt{1+k^2}}\sin(\omega_p t)\sin(2|\alpha|t\sqrt{1+k^2}) + \frac{2k}{(1+k^2)}\cos(\omega_p t)\sin^2(|\alpha|t\sqrt{1+k^2}) \\ -\cos^2(|\alpha|t\sqrt{1+k^2}) + \left(\frac{k^2-1}{k^2+1}\right)\sin^2(|\alpha|t\sqrt{1+k^2}) \end{pmatrix} \quad (4.30a)$$

where

$$k>1 \quad , \qquad k<1 \quad , \qquad k=1/2 \qquad (4.30b)$$

for weak interaction, medium strength interaction and critical (threshold) interaction respectively.

Taking (4.30a) equal to (3.27), we use (3.31) to obtain

$$Tr\hat{\rho}_{-}(t) = 2 - 4\sin^2(|\alpha|t\sqrt{1+k^2}) + 2\sin^4(|\alpha|t\sqrt{1+k^2}) - \frac{(k^2-1)}{(1+k^2)}\sin^2(2|\alpha|t\sqrt{1+k^2}) + \frac{2(k^2-1)^2}{(k^2+1)^2}\sin^4(|\alpha|t\sqrt{1+k^2})$$

$$+\frac{2}{(1+k^2)}\sin^2(\omega_p t)\sin^2(2|\alpha|t\sqrt{1+k^2}) + \frac{8k^2}{(1+k^2)^2}\cos^2(\omega_p t)\sin^4(|\alpha|t\sqrt{1+k^2}) +$$

$$\frac{8k}{(1+k^2)^{\frac{3}{2}}}\sin(\omega_p t)\sin(2|\alpha|t\sqrt{1+k^2})\cos(\omega_p t)\sin^2(|\alpha|t\sqrt{1+k^2}) \qquad (4.30c)$$

At

$$t = \frac{n\pi}{|\alpha|\sqrt{1+k^2}} \quad ; \qquad \text{n=0, 1, 2…} \qquad (4.30d)$$

the trace in (4.30c) is greatest i.e. the trace=2.

For the time

$$t = \left(\frac{1}{2} + n\right)\frac{\pi}{|\alpha|\sqrt{1+k^2}} \qquad \text{n=0, 1, 2…} \qquad (4.30e)$$

the trace in (4.29c) is least i.e.

$$Tr\hat{\rho}_{+}(t) = \frac{2(k^2-1)^2}{(k^2+1)^2} \qquad (4.30f)$$

Where k>1 and the corresponding least trace > 0 under weak interaction, k<1 and corresponding trace =0 and k=1/2 and corresponding least trace is 0.72.

The trace (4.30c) for Bell state vector (3.26b) under weak interaction, medium strength and critical interaction at k>1, k<1 and k=1/2 respectively does not violate the CHSH Bell inequality (3.32) hence a weak entanglement is produced.

.

Entanglement of Bell state vector in (3.26b) for semi-classical OPO under weak interaction, medium strength and critical (threshold) interaction is dynamic and can be best utilized for practical implementation of quantum communication protocols at the time in (4.30d).

We use (4.28) in (4.17c) to obtain

$$\left|\phi_{+}\right\rangle = e^{-i\Omega_{ab}t}\begin{pmatrix} \frac{-i}{\sqrt{1+k^2}}\cos(\omega_p t)\sin(2|\alpha|t\sqrt{1+k^2}) + \frac{2ik}{(1+k^2)}\sin(\omega_p t)\sin^2(\alpha t\sqrt{1+k^2}) \\ \cos(2\alpha t\sqrt{1+k^2}) \\ \cos(2\alpha t\sqrt{1+k^2}) \\ \frac{-i}{\sqrt{1+k^2}}\cos(\omega_p t)\sin(2|\alpha|t\sqrt{1+k^2}) + \frac{2ik}{(1+k^2)}\sin(\omega_p t)\sin^2(|\alpha|t\sqrt{1+k^2}) \end{pmatrix} \quad (4.31a)$$

Taking (4.31a) equal to (3.27), we use (3.31) to obtain the trace of

$\hat{\rho}_{+}(t) = \left|\phi_{+}(t)\right\rangle\left\langle\phi_{+}(t)\right|$ as

$$Tr\hat{\rho}_{+}(t) = 2 - 2\sin^2(2|\alpha|t\sqrt{1+k^2}) + \frac{2}{(1+k^2)}\cos^2(\omega_p t)\sin^2(2|\alpha|t\sqrt{1+k^2}) -$$

$$\frac{8k}{(1+k^2)^{\frac{3}{2}}}\cos(\omega_p t)\sin(2|\alpha|t\sqrt{1+k^2})\sin(\omega_p t)\sin^2(|\alpha|t\sqrt{1+k^2}) +$$

$$\frac{8k^2}{(1+k^2)^2}\sin^2(\omega_p t)\sin^4(|\alpha|t\sqrt{1+k^2}) \qquad (4.31b)$$

where

$$k>1 \quad , \qquad k<1 \quad , \qquad k=1/2 \qquad (4.31c)$$

The trace in (4.31c) is similar to trace in (4.29c). Therefore the entanglement properties for Bell state vector in (3.26c) under weak interaction, medium strength and critical (threshold) interaction when k>1, k<1 and k=1/2 for semi-classical OPO are similar to those of Bell state vector in (3.26a) described above in (4.29d-f).

We use (4.28) in (4.17d) to obtain

$$\left|\phi_{-}\right\rangle = e^{-i\Omega_{ab}t}\begin{pmatrix} \frac{i(\alpha^*(t)-\alpha(t))}{2\alpha\sqrt{1+k^2}}\sin(2\alpha t\sqrt{1+k^2}) - \frac{(\alpha(t)+\alpha^*(t))k}{\alpha(1+k^2)}\sin^2(\alpha t\sqrt{1+k^2}) \\ 1 \\ -1 \\ \frac{i(\alpha(t)-\alpha^*(t))}{2\alpha\sqrt{1+k^2}}\sin(2\alpha t\sqrt{1+k^2}) + \frac{(\alpha(t)+\alpha^*(t))k}{\alpha(1+k^2)}\sin^2(\alpha t\sqrt{1+k^2}) \end{pmatrix} \qquad (4.32a)$$

Taking (4.32a) equal to (3.27), we use (3.31) to obtain the trace of density matrix

$\hat{\rho}\_(t) = \left|\phi\_(t)\right\rangle\left\langle\phi\_(t)\right|$ as

$$Tr\hat{\rho}\_(t) = 2 - 4\sin^2(|\alpha|t\sqrt{1+k^2}) + 2\sin^4(|\alpha|t\sqrt{1+k^2}) - \frac{(k^2-1)}{(1+k^2)}\sin^2(2|\alpha|t\sqrt{1+k^2}) + \frac{2(k^2-1)^2}{(k^2+1)^2}\sin^4(|\alpha|t\sqrt{1+k^2})$$

$$+\frac{2}{(1+k^2)}\sin^2(\omega_p t)\sin^2(2|\alpha|t\sqrt{1+k^2}) + \frac{8k^2}{(1+k^2)^2}\cos^2(\omega_p t)\sin^4(|\alpha|t\sqrt{1+k^2}) +$$

$$\frac{8k}{(1+k^2)^{\frac{3}{2}}}\sin(\omega_p t)\sin(2|\alpha|t\sqrt{1+k^2})\cos(\omega_p t)\sin^2(|\alpha|t\sqrt{1+k^2}) \qquad (4.32b)$$

=

The trace in (4.32b) is similar to the trace in (4.30c). Therefore the entanglement properties for Bell state vector (3.26d) for semi-classical OPO under weak interaction, medium strength and critical (threshold) interaction when k>1, k<1 and k=1/2 are similar to those of Bell state vector in (3.26b) described above in (4.30d-f).

CHAPTER FIVE: CONCLUSION AND RECOMMENDATIONS FOR FURTHER RESEARCH

5.1 Conclusion

5.1.1 Exact solutions of Heisenberg's equations

A semi-classical OPO Hamiltonian was developed in a simplified form (1.5) and used to generate the dynamics of the system through Heisenberg's equations to obtain exact solutions of time evolution equations (3.0). We observe that the Heisenberg's equations are appropriate for determination of exact solutions of time evolution equations and time evolution operators for semi-classical OPO. The time evolution equations were expressed in spin operators and solved through matrix method. This method involved transformation of a Hamiltonian generating the dynamics of the system into a rotating frame through application of unitary transformation operators to produce two forms of time evolving photon polarization operator vectors. Two expressions for time evolution operators, (4.8) and (4.10) were obtained in exact and explicit forms and used to generate general time evolving photon polarization state vectors, (4.11a-d). Expressing Heisenberg's equations in matrix form provides the required exact solutions of time evolution equations which are appropriate for construction of exact and explicit solutions of general time evolving photon polarization state vectors for the horizontal and vertical polarization states.

5.1.2 Bell state vectors

The semi-classical OPO is a suitable system for demonstration of entanglement through exact and explicit solutions of photon polarization state vectors which are easily expressible in exact and explicit time evolving Bell state vectors, (4.17a-d), obtained from the Heisenberg's equations and matrix method.

5.1.3 Test of entanglement of polarization states

Reduced density matrices are appropriate for use in CHSH Bell inequalities as a test for entanglement in the semi-classical OPO. The reduced density matrices are obtained from the

traces of density matrices of polarization state vectors arising from the OPO. It is observed that the entanglement in OPO is dynamic and attainable under all conditions of interaction at varying degrees of entanglement. Entanglement properties were obtained under resonance, very weak interaction, weak interaction, medium strength and critical interaction for the four Bell state vectors.

The traces of Bell state vectors, $|\psi_+\rangle = |H;t\rangle_a |H;t\rangle_b + |V;t\rangle_a |V;t\rangle_b$ and $|\phi_+\rangle = |H;t\rangle_a |V;t\rangle_b + |V;t\rangle_a |H;t\rangle_b$ for semi-classical OPO under resonance and very weak interaction do not violate the CHSH Bell inequality hence producing a dynamically weak entanglement. However, the two Bell state vectors violates the CHSH Bell inequality under weak interaction, medium strength interaction and critical interaction producing a strong entanglement. The traces of Bell state vectors $|\psi_-\rangle = |H;t\rangle_a |H;t\rangle_b - |V;t\rangle_a |V;t\rangle_b$ and $|\phi_-\rangle = |H;t\rangle_a |V;t\rangle_b - |V;t\rangle_a |H;t\rangle_b$ under resonance violates the CHSH Bell inequality to obtain S=4 forming a dynamic stronger entanglement beyond the Cirel'son's inequality of a maximum projection of $S< 2\sqrt{2}$ for quantum theory. Thus, entanglement obtained in the OPO is the strongest ever achieved for continuous quantum variables from violation of Bell inequalities hence the OPO is a potential system proposed for practical implementation of quantum communication protocols in quantum mechanics.

.

All the four Bell state vectors do not violate the CHSH Bell inequality under very weak interaction hence a weak entanglement which is dynamic in nature is produced.

The CHSH Bell inequality is violated to give a higher trace of 4 under resonance, weak interaction, medium strength and critical interaction hence producing a stronger entanglement. The semi-classical OPO is a good system for demonstration of entanglement of polarization states by use of Bell states. Heisenberg's equations and matrix method are appropriate for study of polarization states in the OPO to produce dynamic evolution of entanglement with greatest entanglement produced at the time (4.20d) and (4.29e).

5.2 Recommendations for further research

We have shown high degree of entanglement in the OPO in an elaborate manner through exact and explicit solutions of time evolution operator and Bell states obtained directly through Heisenberg's equation using simpler matrix-based method under all conditions of interaction. The photon polarization state vectors from the OPO are therefore essential in quantum technology. From entanglement results obtained in the semi-classical OPO, further research can be done by developing quantum communication protocols such as teleportation, quantum key distribution and quantum computing, at the time (4.20d) and (4.29e) for the four Bell state vectors which have produced greater degree of entanglement specifically under resonance, weak interaction, medium strength and critical interaction within the semi-classical OPO.

REFERENCES

Adams W. (2016). *China's Quantum Cryptography: Tales from (Quantum) Crypt.* National law-review. http://www.natlawreview.com/article/china-s-quantum-cryptography-tales-quant -crypt. accessed on 5/2/2017.

Akeyo J.O. (2008). *Revisiting non-degenerate parametric down-conversion*. Pramana-journal of physics Vol. 71, No. 6 pp. 1311-1320.

Anand K. (2009). *Coherence Properties of the Entangled Two-Photon Field Produced by Parametric Down-Conversion*. Hajim School of Engineering and Applied Sciences University of Rochester Rochester, New York. www.optics.rochester.edu/workgroups/boyd/ assets/pdf/.../Phd Thesis jha.pdf. accessed on 2/4/2015.

Bass M. (2001). *Fiber Optics and Nonlinear Optics*: Volume IV. Optical Parametric Oscillators New York: McGraw-Hill (2nd ed., PP. 22-1 – 22-65) Applied optics 40,5446-5451.

Bell J. (1964). *On the Einstein-Podolsky-Rosen paradox*. Physics1,195-200.

Bennett H. and Brassard G. (1993). "*Teleporting an unknown quantum state via dual classical and Einstein-Podolsky-Rosen channels*". Phys. Rev. Lett. 70, 1895.

Bennett H. and Wiesner S. (1992). "*Communication via one- and two-particle operators on Einstein-Podolsky-Rosen states,* "Phys. Rev. Lett. 69, 2881.

Boto A. and Kok P. (1994). "*Quantum interferometric optical lithography: Exploiting entanglement to beat the diffraction limit***,"** Phys. Rev.Lett.85,2733.

Chakrabarti R. and Jenisha J. (2015). *Quasi-Bell states in a strongly coupled qubit-oscillator system and their delocalization in the phase space*. Phys.Rev.lett.88,148301.

Chauser J. and Shimony A. (1978). *Quantum mechanics* Rep. Prop. Physics. Vol 30. No. 2.

Coutinho B. and Santos D. (2005). "*Quantum analysis of the nondegenerate optical parametric oscillator with injected signal*", Phys. Rev. A 72, 033820.

Eberhard P. H. (1999). *Violation of Bell's inequality*. Phys. Rev.A., 60, RR773.

Ekert A. (1991). "*Quantum cryptography based on Bell's theorem*," Phys. Rev. Lett. 67, 661.

Fujii K. (2003). *Two-level system and some approximate solutions in the strong-coupling regime***.** http://arxiv.org/pdf/quant-ph/0301145V2. accessed on 4/2/2016.

Giordmaine J. and Miller R. (1965). "Tunable coherent parametric oscillation in LiNb03 at optical frequencies". Phys. Rev. Lett. APS. 14: 973. Bibcode: 1965PhRvL..14..973G. doi: 10. 1103/PhysRevLett. 14.973.

Herbst V. and Scheidl F. (2012). "*Quantum teleportation over 143 kilometers using active feed-forward*"**.** Bibcode: Nature 489.,269M.doi:10.1038/nature 11472.

Jin L. and Martinez A. (2013). *Optimization of output power in a fiber optical parametric oscillator***.** Opt Express.23;21(19):22617-27. doi: 10.1364/OE.21.022617.

Johansson R. (2014). *Entangled-state generation and Bell inequality violations in nanomechanical resonators*. Phys. Rev. B90, 174307.

Kenta T. and Yoshihisa Y. (2015). *Quantum correlation in degenerate optical parametric oscillators with mutual injections*. Phys. Rev. A92, 043821.

Kingston H. (1962). "*Parametric amplification and oscillation of optical frequencies*", Proc. IRE 50, 472–474.

Kwiat P. and Mattle K. (1995). *New high-intensity source of polarization-entangled photon pairs*. Phys.Rev. Lett. 75, 4337.

Kwiat P. and Waks Y. (1999). *Ultrabright source of polarization-entangled photons***.** Phys. Rev. A 60, R773R776.

Ling A. (2008). *Entangled state preparation for optical quantum communication*. National university of Singapore. http://www.quantumlah.org/media/thesis-alex.pdf. accessed on 3/7/2015.

Matteo B. (2014). *Entanglement generation in the ultra-strongly coupled Rabi model*. http://arxiv.org/abs/1410.6380V1. accessed on 14/4/2015.

Munro W. J., Nemoto K. and White A. G. (2001). *The Bell inequality: a measure of entanglement.* Journal of Modern Optics, Vol. 48, No. 7, 1239-1246.

Pereira F. and Kimble J. (1992). "*Realization of the Einstein-Podolsky-Rosen Paradox for Continuous Variables*", Phys. Rev. Lett. 68, 3663–3666.

Popescu S. (1994). *Bell inequality*. Phys. Rev. Lett., 72,797.

Preskil J. (1998). *Quantum information and computation*: Lecture Notes for physics 229. California. http://www.lorentz leidenuniv.ni/quantum computers/preskill/ph. accessed on 21/4/2015.

Reid M. Drummond P. (1989). *"Correlations in nondegenerate parametric oscillation-squeezing in the presence of phase diffusion,"* Phys. Rev. A 40, 4493-4506.

Rekdal P. and Skagerstam B. (1999). *Quantum dynamics of non-degenerate parametric* amplification.http://arxiv.org/abs/quantph/9910007V1.DOI:10.1238/physica.scripta 61 296. accessed on 26/5/2015.

Rice R. (2005). *Entanglement, Teleportation, and single photon storage using two level atoms inside an Optical Parametric Oscillator*. http://arxiv.org/pdf/quant-ph/0508198V1. accessed on 2/3/2015.

Rubin M. and Klyshko L. (1994). *Photons and Nonlinear Optics***.** D. N. Klyshko, Gordon and Breach Science, New York. D. A. Phys. Rev. A 50, 5122.

Rupert U. (2004). *"Quantum teleportation across the Danube*". http://www.nature.com/ articles/430849a/doi:10.1038/430849a. accessed on 6/7/2014.

Shahrokhshahi R.and Pfister O. (2012). *Large-scale multipartite entanglement in the quantum optical frequency comb of a depleted-pump optical parametric oscillator*. http://arxiv.org/pdf/1110.6450v2. accessed on 12/6/2015.

Su X. and Tan A. (2006). ‘*’Experimental demonstration of quantum entanglement between frequency-nondegenerate optical twin beams*," Opt. Lett. 31, 1133.DOI:10.1364/OL.

Takeda T. (2014).*"Deterministic quantum teleportation of photonic quantum bits by a hybrid technique*"**.** Arxiv.14024895(quant-ph).Nature 500, 315. DOI: 10.1038/nature 12366.

Villar S. and Cassemiro N. (2006). *Entanglement in the above-threshold optical parametric oscillator*. http://arxiv.org/pdf/quant-ph/0610208. accessed on 2/2/2015.

Villar S. and Cassemiro, N. (2005). ‘*’Generation of Bright Two-Color Continuous Variable Entanglement*," Phys. Rev. Lett. 95, 243603.

Wendin G. and Shumeiko V. (2005). *Superconducting quantum circuits, qubits and computing*. http://arxiv.org/abs/cond-mat/0508729. accessed on 12/7/2015.

Yurke B. and Stoler D. (1992). "*Einstein-Podolsky-Rosen from independent particle sources*," Phys. Rev. Lett. 68, 1251.